



UNIVERSITY OF LEEDS

This is a repository copy of *Stratigraphic architecture of back-filled incised-valley systems: Pennsylvanian–Permian lower Cutler beds, Utah, USA*.

White Rose Research Online URL for this paper:
<http://eprints.whiterose.ac.uk/80267/>

Version: Accepted Version

Article:

Wakefield, OJW and Mountney, NP (2013) Stratigraphic architecture of back-filled incised-valley systems: Pennsylvanian–Permian lower Cutler beds, Utah, USA. *Sedimentary Geology*, 298. 1 - 16. ISSN 0037-0738

<https://doi.org/10.1016/j.sedgeo.2013.10.002>

Reuse

Unless indicated otherwise, fulltext items are protected by copyright with all rights reserved. The copyright exception in section 29 of the Copyright, Designs and Patents Act 1988 allows the making of a single copy solely for the purpose of non-commercial research or private study within the limits of fair dealing. The publisher or other rights-holder may allow further reproduction and re-use of this version - refer to the White Rose Research Online record for this item. Where records identify the publisher as the copyright holder, users can verify any specific terms of use on the publisher's website.

Takedown

If you consider content in White Rose Research Online to be in breach of UK law, please notify us by emailing eprints@whiterose.ac.uk including the URL of the record and the reason for the withdrawal request.



eprints@whiterose.ac.uk
<https://eprints.whiterose.ac.uk/>

Stratigraphic architecture of back-filled incised-valley systems: Pennsylvanian-Permian lower Cutler beds, Utah, USA

OLIVER J. W. WAKEFIELD^{1,2} and NIGEL P. MOUNTNEY³

1 – Former address: Earth Sciences and Geography, Keele University, Staffordshire ST5 5BG, UK

2 – British Geological Survey, Keyworth, Nottingham, NG12 5GG, UK Email: oliverw@bgs.ac.uk (corresponding author)

3 – School of Earth and Environment, University of Leeds, Leeds LS2 9JT, UK. Email: n.mountney@see.leeds.ac.uk

Abstract

The Pennsylvanian to Permian lower Cutler beds collectively form the lowermost stratigraphic unit of the Cutler Group in the Paradox Basin, southeast Utah. The lower Cutler beds represents a tripartite succession that comprises lithofacies assemblages of aeolian, fluvial and shallow-marine origin, in near equal proportion. The succession comprises a series of transgressive-regressive cycles, the origin of which was driven by repeated episodes of climatic variation and linked changes in relative sea-level. Cyclic variations in relative sea-level were responsible for the creation and subsequent infill of a series of incised valley systems. Incised valley creation occurred as a lowering of base-level, associated with relative sea-level fall, initiated incision within the fluvial system. Fluvial incision occurred during falling-stage and lowstand episodes within each relative sea-level cycle. Subsequent relative sea-level rises resulted in the back-flooding of these incised-valley systems and their infill via shallow-marine and estuarine processes. Back-flooded valley systems generated marine embayments within which additional local accommodation was exploited. Back-filling is characterised by a distinctive suite of lithofacies arranged into a lowermost, basal fill of fluvial channel and overbank architectural elements, passing upwards into barform elements with indicators of tidal influence, including inclined heterolithic strata and reactivation surfaces. The incised-valley fills are capped by laterally extensive and continuous marine limestone elements that record the drowning of the valleys and, ultimately, flooding and accumulation across surrounding interfluves (transgressive surface). Limestone elements are characterised by an open-marine fauna and represent the preserved expression of maximum transgression. These back-filled incised valley systems represent a type of shallow-marine and shoreline succession that has hitherto received little detailed study regarding sedimentary response to a complex set of coeval autogenic and allogenic processes.

Keywords: incised valley; transgression; base-level; accommodation; shoreline

1 Introduction

Although many previous studies have examined the sedimentary style of modern and ancient depositional systems developed in arid regimes in which aeolian and fluvial sedimentary environments undertook a variety of styles of interaction (e.g. Langford and Chan, 1988; 1989; Stanistreet and Stollhofen, 2002; Mountney and Jagger, 2004), relatively few have examined tripartite styles of interaction involving coastal settings where aeolian, fluvial and shallow-marine processes all operated coevally (e.g. Simpson and Eriksson, 1993; Blakey et al., 1996). One system for which the regional stratigraphic record of such tripartite interactions is now relatively well documented is the Pennsylvanian to Permian lower Cutler beds of the Paradox foreland basin, southeast Utah (Rankey, 1997), a coastal desert system whose development was influenced by high-frequency changes in climate from arid to sub-humid, and associated changes in relative sea-level driven by glacio-eustasy (Jordan and Mountney, 2010; 2012). Within these repeated episodes highstands can be demonstrably linked to phases of increased climatic humidity, whereas lowstands equate to relatively more arid climatic phases (Jordan, 2006). Related styles of interaction are also identified in other formations of the Paradox Basin (Loope, 1985; Atchley and Loope, 1993; Dickinson et al., 1994; Goldhammer et al., 1994; Rankey, 1997; Jagger, 2003; Mountney and Jagger, 2004; Jordan, 2006; Mountney, 2006b; Jordan and Mountney, 2010; 2012), and also from other Permian basins of North America (Heckel, 1980; Dickinson et al., 1994; Soreghan, 1994; Blakey, 2008).

Initial studies of the lower Cutler beds (Terrell, 1972; Mack, 1978; Loope et al., 1990; Jordan, 2006) were principally concerned with determination of the regional palaeogeographical setting and stratigraphic framework of the succession. As such, the succession is characterised by multiple, 10 to 20 m-thick repeating cycles of sandstone and limestone units (e.g. Terrell, 1972; Mack, 1978). Of these the uppermost 10 to 12 cycles are accessible in tributary canyons of the Colorado River. Loope (1984) convincingly demonstrated that the majority of the sandstone-dominated units in the succession were of continental aeolian and fluvial origin, whereas the bioclastic limestone units were of shallow-marine origin; the succession is therefore considered to record a series of transgressive-regressive events. Loope (1985) suggested that the preserved cycles might have arisen as a result of Milankovitch-style orbital forcing and proposed a ~413 kyr duration for each. The relationship between sandstone units of continental origin and limestone units of marine origin establish a model framework to account for stacked depositional cycles attributed to relative sea-level change (Rankey, 1997). Thin but laterally extensive and continuous marine

Version: Final draft**Updated:** 18/04/2013 12:13:45

limestone units present within each cycle have been traced by Jordan and Mountney (2010; 2012) from locations indicative of relatively more off-shore depositional settings to those indicative of relatively more landward settings. They thin and eventually pinch-out defining the maximum transgression of each relative sea-level cycle; these units and other key stratal surfaces define the basis for a sequence stratigraphic framework for the lower Cutler beds (Jordan, 2006; Jordan and Mountney, 2010; 2012). Within this framework, 12 cycles record evidence for transgression, regression and sequence boundary generation in response to rising and falling relative sea-level and associated changes in climate (Jordan and Mountney, 2010; 2012); thus, the cycles define sequences *sensu* Van Wagoner et al. (1990).

During episodes of falling relative sea-level the palaeo-shoreline shifted in excess of 80 km basinward. This allowed fluvial systems to extend across a low-gradient coastal plain to reach new lowstand shorelines and, in doing so, cut a series of incised valley systems. These were later back-filled during subsequent transgression associated with relative sea-level rise at commencement of the next sequence. Hitherto, there have been no published accounts of the detailed geometry of these incised-valley systems or the sedimentary architecture and palaeoenvironmental significance of the infill for the lower Cutler beds.

The aim of this study is to document the mechanisms responsible for the generation of a series of incised-valley systems in the lower Cutler beds, and to establish the timing of incision in relation to base-level fall and sedimentary style of back-filling during subsequent base-level rise. Specific objectives of this study are as follows: (i) to document the preserved sedimentological and architectural relationships between lithofacies assemblages of aeolian, fluvial and shallow-marine origin within and adjacent to the incised-valley systems; (ii) to demonstrate how interactions between coeval fluvial, shoreline and shallow-marine processes led to incised-valley formation and infill during one complete cycle of relative sea-level change; (iii) to discuss the climatic and eustatic conditions required to generate the preserved stratigraphic architectural relationships within the context of a sequence stratigraphic model.

This study is important for the following reasons: (i) it enables an understanding of the nature of interactions between competing coeval fluvial, aeolian and shallow-marine systems in shoreline settings; (ii) it allows determination of sedimentary response to base-level change and climatic shifts driven by glacio-eustasy in arid shoreline settings; (iii) it demonstrates a linkage between the origin of incised-valley systems generated during base-level fall and their back-filling during subsequent base-level rise.

2 Geological Setting

2.1 The Paradox Basin

The Pennsylvanian to Permian lower Cutler beds represent the basal-most lithostratigraphic unit of the Cutler Group in the Paradox Basin, southeast Utah (figure 1). The Paradox Basin formed as a result of growth of the Uncompahgre Uplift to the northeast, which initiated subsidence in the foreland due to flexural lithospheric loading (Condon, 1997; Barbeau, 2003; figure 2). The basin has an asymmetric oval morphology with a northwest-southeast-oriented long axis that is ~320 km in length and a perpendicular short axis that is ~150 km wide (Condon, 1997). The limits of the basin generally defined by the maximum lateral extent of halite and potash salt deposits that occur in the middle Pennsylvanian Paradox Formation of the Hermosa Group, which underlies the Cutler Group (Kunkel, 1958; Campbell, 1980; Blakey and Knepp, 1989; Nuccio and Condon, 1996; Condon, 1997; Barbeau, 2003). However, throughout much of its evolution, the Paradox Basin developed in an overfilled state and many of the formal stratigraphic units associated with the basin, including the lower Cutler beds, extend considerably beyond the defined boundaries (Blakey et al., 1996; Condon, 1997). Overfilling likely resulted from slower rates of accommodation space creation (Barbeau, 2003), which in turn promoted a basinward progradation of a large wedge of clastic detritus of continental origin from the Uncompahgre Uplift (Loope, 1984). Subsidence rates within the Paradox Basin during the deposition of the lower Cutler beds are considered relatively constant (Nuccio and Condon, 1996); as such, allowing any variations in preserved sedimentary expression to be attributed directly to variations in linked climatic and relative sea-level forcing.

The Uncompahgre Uplift served as the principal sediment source area during the episode of accumulation represented by the lower Cutler beds. A series of fluvial systems drained into the Paradox Basin, with detritus delivered via alluvial fans and braided river systems that generally flowed south-westwards from the uplift (Nuccio and Condon, 1996; Condon, 1997; Jordan and Mountney, 2010). In the central part of the basin, distal to the fluvial-dominated foredeep region adjacent to the Uncompahgre Uplift, aeolian dune-field systems developed, with bedforms that migrated south-eastwards along the long-axis of the basin. The sediment for aeolian bedform construction was probably derived from pre-existing fluvial and coastal deposits in the north-western part of the basin (figure 2; Condon, 1997; Blakey, 2009). The aeolian dune field and its envisaged source system were bounded to the west and southwest by a shallow-marine seaway that transgressed and regressed over the coastal plain and inland across a low-relief alluvial plain. This had an impact upon the supply of sediment to the aeolian system and dictated its availability for aeolian transport; ultimately

Version: Final draft**Updated:** 18/04/2013 12:13:45

governing the timing of aeolian dune-field construction and deflation (cf. Kocurek, 1999; Kocurek and Lancaster, 1999; Mountney, 2012). The shallow-marine system was characterised by mixed siliciclastic and carbonate sedimentation in a gently-inclined ramp setting (Jordan, 2006; Jordan and Mountney, 2010). A varied marine faunal assemblage including brachiopods, bivalves, crinoids and bryozoans indicates open marine conditions (Terrell, 1972).

2.2 The lower Cutler beds

The “lower Cutler beds” is the informal name assigned to the lowermost strata of the Cutler Group that underlie the Cedar Mesa Sandstone in the central part of the Paradox Basin (Loope, 1981; Stanesco and Campbell, 1989; Loope et al., 1990). The adoption of this name avoids confusion associated with prior nomenclature in which the succession was variously called the Rico Formation (McKnight, 1940) or the Elephant Canyon Formation (Baars, 1962; 1979) – see discussion of Loope et al. (1990) for details. The name “lower Cutler beds” is now generally accepted by most modern studies (Condon, 1997; Stanesco et al., 2000; Jordan and Mountney, 2010; 2012) and is therefore used in this study. The lower Cutler beds overlie the Honaker Trail Formation – the uppermost unit of the Hermosa Group (Williams, 1996) – and are conformably overlain by the Cedar Mesa Sandstone of predominantly aeolian dune and interdune origin (Loope, 1984).

The lower Cutler beds are characterised by a series of 10 to 20-m-thick repeating cycles of sandstone and limestone. In the north-eastern part of the Paradox Basin, close to the Uncompahgre Uplift, the marine limestone units of the lower Cutler beds thin and pinch-out at a position where the unit passes laterally into the exclusively non-marine succession of the so-called “undifferentiated” Cutler Group (Mack and Rasmussen, 1984; Nuccio and Condon, 1996; Jordan and Mountney, 2010), a succession characterised by an up to 4000-m thick wedge of alluvial detritus that was shed from the evolving Uncompahgre Uplift into the foredeep of the Paradox Basin (Mack, 1977; Kluth and Duchene, 2009; Rasmussen and Rasmussen, 2009; Trudgill, 2011).

Overall, the lower Cutler beds accumulated in a near-shore coastal plain and littoral setting, within which sedimentation was influenced by aeolian, fluvial and shallow-marine processes (Rankey, 1997). Lithofacies accumulated under the influence of a variable arid to sub-humid climate, changes of which were driven by global switches between icehouse and greenhouse conditions (Loope, 1985). Studies of relationships between lithofacies assemblages and the architectural elements that they define have led to the erection of a sequence stratigraphic framework for the succession (Rankey, 1997; Jordan and Mountney, 2010; 2012). Within this framework depositional cycles, comprised of repeated successions

Version: Final draft**Updated:** 18/04/2013 12:13:45

of aeolian, fluvial and shallow-marine elements, equate to sequences driven by relative sea-level changes (Jordan and Mountney, 2012). Significantly, changes in both climate and relative sea-level can be shown to be related, whereby episodes of relative sea-level lowstand occurred at times of increased climatic aridity, whereas highstand conditions relate to episodes of increased climatic humidity (also see Soreghan et al., 2002).

Within these preserved cycles, bioclastic limestone elements associated with marine transgression are thin (<1 to 10 m) but highly continuous and regionally correlatable over an area > 5000 km², demonstrating that the coastal plain over which transgressions progressed lacked significant relief and dipped seaward at a low angle. The low-gradient and low-relief nature of the coastal plain meant that even modest (~20 m) changes in relative sea-level induced dislocations in the position of the palaeo-coastline over distances of in excess of 80 km (Jordan and Mountney, 2010; 2012).

Although previous work has established a detailed stratigraphic framework for the lower Cutler beds (Terrell, 1972; Mack, 1977; 1978; Jordan, 2006; Jordan and Mountney, 2010; 2012), the geometry and internal sedimentary architecture of a series of incised valley-fill systems identified in parts of this formation have hitherto not been described. Accounting for their detailed origin provides the opportunity to develop a generic model which places these distinctive features in a sequence stratigraphical context.

3 Data Collection and Field Locations

Incised valley systems defined by major incision surfaces and their infills in the lower Cutler beds are well-exposed in natural outcrops formed by the canyon walls of the present-day Colorado River and its tributaries in Canyonlands National Park and in Indian Creek (figure 3). Cliff-forming sections arranged in a variety of orientations expose the upper 50 to 80 m of the lower Cutler beds at three main study localities, each situated ~30 km apart: Little Spring Canyon, Indian Creek and the Shafer Basin (figure 3).

A series of two-dimensional architectural panels (the locations of which are shown in figure 3) arranged in a variety of orientations record a >2,200 m-long and 40 to 70 m-thick part of the succession for the Indian Creek and Shafer Basin field localities. These panels form the basis for a pseudo-three-dimensional representation of the geometries of the architectural elements present and their relationship to key stratal surfaces. Data are recorded on scaled architectural diagrams calibrated to 24 measured sedimentary log sections. Each architectural panel records the two-dimensional geometry of the elements present, including their lateral and vertical extent, their style of juxtaposition relative to one another, and indicators of palaeocurrent (206 readings in total) recorded from features such as trough

Version: Final draft**Updated:** 18/04/2013 12:13:45

cross-bedding. Individual panels detailing adjoining parts of the stratigraphy have been arranged to form composite panels, and are depicted in orientations that mimic the trend of the outcrop pattern, thereby allowing insight to be gained into the three-dimensional geometry of the various architectural elements and their bounding surfaces (figure 3). Additionally, eighteen high-resolution sedimentary logs spaced ~25 m apart have been taken from the field locality at Little Spring Canyon and used to construct a fence panel that records the observed architectural elements along a ~450 m-long and ~40 m-thick cliff-section (figure 3).

The accessible uppermost part of the lower Cutler beds exposes twelve (Jordan, 2006) vertically stacked 1 to 20 m-thick sequences (cycles), each composed of associations of facies of aeolian, fluvial and shallow-marine origin that define architectural elements. Each sequence is marked at its top by a bioclastic marine limestone or granulestone unit, the uppermost surface of which represents a sequence boundary, with evidence for subaerial exposure of marine deposits in the form of karstic surfaces and palaeosols (Jordan and Mountney, 2010). This forms the basis for the sequence stratigraphic framework, which enables the architectural panel data discussed here to be placed within a regional context. Using the sequence nomenclature of Jordan and Mountney (2012), maximum flooding surfaces FS9, FS10, FS11 and FS12 are identified.

4 Architectural elements

A series of distinctive architectural elements form the smaller-scale building blocks of the infills of the incised valley systems. Several previous studies have outlined comprehensive lithofacies and architectural element schemes for the lower Cutler beds (Terrell, 1972; Mack, 1977; Langford and Chan, 1988; Condon, 1997; Soreghan et al., 2002; Jordan, 2006; Jordan and Mountney, 2010; 2012). As such, only summary descriptions of architectural elements are included here. Table 1 and figure 4 summarize and depict principal lithofacies types; figures 5 to 9 depict common and significant architectural elements and their relationship to each other within the context of the infills of studied incised valley systems.

4.1 Aeolian dune element

Description. Sets of planar and trough cross-strata that are composed internally of grainflow and grainfall strata (facies A1 and A3 respectively, table 1; Hunter, 1977), examples of which downlap onto basal set boundaries or commonly interfinger with and grade into near-horizontal wind-ripple laminations in the basal parts of sets. Cross-bedded sets are 1 to 5 m thick and occur as tabular inclined bodies that extend laterally for 100s of metres in directions both parallel and perpendicular to migration. Sets are gently inclined at angles of

Version: Final draft**Updated:** 18/04/2013 12:13:45

<2° relative to the depositional palaeo-horizontal and are commonly vertically stacked to form compound cosets. Vertically-stacked sets and cosets of dune elements are commonly separated by interdune elements (see below). Where aeolian dune elements occur at the top of an aeolian succession, they are commonly characterized by laterally extensive horizontal and planar bounding surfaces that can be traced for many kilometres and which truncate all internal structures; such bounding surfaces typically have rhizoliths associated with them (figure 5).

Interpretation. These tabular cross-bedded sets and cosets are the product of the accumulation of migrating aeolian dunes that possessed active slipfaces inclined at or near the angle of repose (Hunter, 1977; 1981; Rubin and Hunter, 1983). Trough cross-bedded sets denote bedforms that possessed sinuous along-crest morphologies (Rubin, 1987; Mountney, 2006a). Stacked aeolian dune elements represent deposits of an aeolian dunefield system for which conditions were favourable for accumulation (cf. Lancaster, 1983; Kocurek, 1999). The laterally extensive, horizontal bounding surfaces that truncate these elements are deflationary supersurfaces (Loope, 1985; Mountney, 2012). These supersurfaces record an episode of dune-field destruction brought about by an upwind reduction in availability of sediment for aeolian transport, leading to downwind cannibalisation of the dune field to the level of the water table by winds that were under-saturated with respect to their potential sand carrying capacity (see Loope, 1985; Langford and Chan, 1988; 1989).

4.2 Aeolian interdune element

Description. Aeolian interdune elements form lens-shaped bodies from 0.1 to 2.5 m thick and have lateral extents up to 250 m in sections orientated both parallel and perpendicular to the maximum dip-azimuth of foresets in adjoining cross-bedded dune elements. Lithofacies present include (see table 1) aeolian wind-ripple strata (A2), massive sandstone (F7), wavy and convolute sandstone (F8) and laminated siltstone (F6). These elements occur in close association with and are commonly encased by aeolian dune elements.

Interpretation. The occurrence of these elements between aeolian dune elements, together with their internal facies compositions, demonstrates an interdune origin, whereby these elements represent deposition in the flat areas between migrating aeolian dunes (Mountney and Thompson, 2002; Mountney, 2012). Aeolian interdunes composed exclusively of aeolian wind-ripple strata had dry substrates, whereas those composed of massive sandstone record episodes of short-lived flash flood events along interdune corridors (cf. Langford and Chan, 1989; 1993; Bullard and Livingstone, 2002; Mountney and Jagger, 2004; Cain, 2009) in a style similar to that in many present-day dune fields (Lancaster, 1983; Langford, 1989;

Tooth, 1999; Stanistreet and Stollhofen, 2002; Krapf et al., 2003; 2005). These massive sandstone sets are of fluvial origin and are differentiated from similar sets of aeolian origin by virtue of their diagnostic red-brown colour, occurrences of rare intraformational rip-up clasts and, in some cases, increased mica content. Interdune flooding could have resulted from coalescing of water in the aftermath of a rain storm within the dune field itself, or could arise in response to fluvial incursion from outside the dune field (figure 6). Interdune elements composed of wavy- and convolute-bedded sandstone and laminated siltstone most likely represent soft-sediment deformation of interdune deposits in the presence of an elevated water-table (Doe and Dott Jr, 1980; Kocurek, 1981; Horowitz, 1982).

4.3 Fluvial channel element

Description. Elongate channel-shaped bodies observed in sections perpendicular to fluvial palaeoflow direction have thicknesses of 2 to 5 m and individual storeys have widths of 10 to 30 m. In sections parallel to palaeoflow these elements have lateral extents of many hundreds of metres to a few kilometres. Examples of these elements have prominent erosional basal bounding surfaces and typically have a horizontal, sharp well-defined upper bounding surface. These elements occur as isolated features or as collections of genetically-related storeys that are vertically and laterally stacked in a multi-storey or multi-lateral style. Internally, these elements are characterised by pebble-rich sandstone facies (F2) containing predominately of local origin with some rare extra-basinal clasts of mafic and ultra-mafic composition, sets of cross-bedded sandstone facies (F1) up to 5 m thick, horizontally laminated sandstone facies (F3) and ripple-laminated sandstone facies (F4).

Fluvial channel elements arranged as multi-storey, multi-lateral complexes typically directly overlie aeolian dune elements. Examples of isolated, individual channel elements may occur nested within successions of predominately aeolian origin (figure 5). Fluvial channel elements are also associated with marine elements in mixed fluvial and marine parts of the succession (discussed later). Examples of such fluvial-marine channel elements occur laterally adjacent to and grade into granulestone barform elements (see below); both element types exhibit large-scale (up to 5 m high), low-angle-inclined (10 to 15°) dipping surfaces that form perpendicular to the flow direction indicated by the small-scale dune cross-bedding.

Interpretation. Geometries and constituent facies types of this element (table 1) are consistent with an interpretation as a fluvial channel body. The lower erosional bounding surface records the cut of the channel and the sharp upper surface records an apparently abrupt cessation in infill, probably associated with abandonment related to the short-lived, ephemeral nature of the fluvial processes in desert systems (Langford and Chan, 1989). The

vertical or lateral overprinting of channel elements indicates multiple, separate episodes of fluvial channel scour and fill into pre-existing relict fluvial channel elements and signifies repeated episodes of flooding. Fluvial channel elements that occur in close association with granulestone barform elements record the mixing of fluvial and shallow-marine processes, within in a tidally influenced setting (see below) where channel elements became established as longer-lived features that undertook lateral accretion, as demonstrated by the presence of large-scale, low-angle-inclined surfaces (figure 7).

4.4 Fluvial overbank element

Description. Tabular and lens-shaped bodies that are 0.3 to 1.6 m thick and have lateral extents up to 500 m in directions both parallel and perpendicular to fluvial flow are common (figure 8). Such elements are commonly truncated by fluvial channel elements with which they are closely associated. This element contains lithofacies of horizontally laminated sandstone (F3), ripple laminated sandstone (F4), laminated siltstone (F6) and calcrete-rich sandstone (F5), each commonly hosting poorly developed palaeosols; successions of facies occur in an overall upward-fining trend within the element. Calcrete palaeosols with calcified rhizoliths (cf. Loope, 1988) are commonly present in the uppermost parts of these elements and these overprint original primary lithofacies types. Tubular, unlined, predominately straight trace fossils up to 6 mm in width and up to 60 mm in length are present along sandstone bedding surfaces within this element. Vertically stacked arrangements of multiple instances of these elements are common, with each element characterised by a fining-upward trend, many examples being capped by palaeosols and rhizoliths. These elements typically occur in the upper portions of fluvially-dominated parts of sequences, where they overlie amalgamated fluvial channel elements. More rarely, examples of this element also exist between stacked fluvial channel elements, though typically as remnant fragments. These elements are commonly overlain by isolated channel elements or, where they form stacked composite elements, may have isolated channel elements nested within them.

Interpretation. This element represents accumulation from non-channelised flow across floodplains at times when the capacity of existing channels to contain flood waters had been exceeded (Tooth, 1999; 2000; 2005). The rapid dissipation of energy associated with a change from channelised to non-channelised flow resulted in deposition proximal to the active channel on the alluvial plain.

4.5 Marine limestone element

Description. Bioclastic, micritic limestone (locally composed of mixed carbonate and siliciclastic facies) occurs as tabular, sheet-like elements that are 1 to 4 m thick and have lateral extents that can be traced, where not locally removed by erosion at the base of the

overlying sequence, for tens of kilometres with little appreciable change in element thickness (Jordan and Mountney, 2012). Abundant diagnostic bioclasts include broken fragments of brachiopods, bivalves, bryozoans, crinoids and corals, with *Scolicia* and *Planolites* abundant on some bedding surfaces.

In places, examples of this element are underlain gradationally by granulestone barform elements (figure 9), in which case mixed siliciclastic-carbonate facies form the basal component of the element and such deposits are appreciably coarser grained, being composed of coarse sand to granulestone quartz and feldspar clasts (up to 30%). Marine limestone elements are overlain either by granulestone barform elements which are locally erosive into the underlying limestone element, or by fluvial overbank or channel elements, in which case the limestone elements exhibit a weathered upper surface that in places grades vertically into immature palaeosols facies. Though marine limestone elements may occur at any level within a marine succession, they are most commonly observed as the uppermost marine element. Marine limestone elements contain bioclastic limestone facies (M1) and siliciclastic-rich limestone facies (M2) types.

Interpretation. Limestone elements represent accumulation in a shallow-marine, carbonate environment in which siliciclastic input from the adjacent terrigenous environment was generally abundant. The lack of appreciable change in thickness for this element over thousands of square kilometres demonstrates that the twelve limestone elements likely accumulated in an environment that lacked any significant break of slope (cf. Tucker and Wright, 1990; Jordan, 2006). Vertical gradation into palaeosol facies is interpreted as the product of subaerial exposure and weathering of the limestone (Wright, 1994).

4.6 Granulestone Barform element

Description. Granulestone barform elements either form tabular sheet-like bodies that have thicknesses of 0.5 to 3 m and lateral extents of several hundred metres, or they occur as erosively-based channelised elements with thicknesses up to 10 m and cross-sectional lateral extents from 20 to 200 m. Both types of barform are comprised of the same facies types (M3 and M4; table 1), though sheet-like forms of the element often contain fewer and smaller pebble clasts. Typically the pebble-grade clasts in facies M3 account for 20 to 25 % of the population, but within the sheet-like element it is typically less than 10% and here pebbles tend to be smaller (rarely exceeding 16 mm diameter, compared to a maximum of ~40 mm found in the channelised version of this element). The basal component of granulestone barforms typically contains abundant marine bioclast fragments that grade upward into a fossiliferous grainstone or packstone lithofacies, with an overall fining-upward trend and a siliciclastic component of up to 25% by volume.

Version: Final draft**Updated:** 18/04/2013 12:13:45

Channelised granulestone barforms typically form vertically and laterally overlapping stacked amalgamated geometries. Individual barforms of this type commonly exhibit trough-crossbedding on a range of scales (0.5 – 7 m) in complicated sets where smaller crossbeds occur within sets compartmentalised by bounding surfaces of large crossbed sets. Crossbedded sets (of all scales) commonly contain inclined surfaces that truncate individual crossbeds but do not extend beyond the set bounding surfaces.

Large (up to 40 m-long) sigmoidal surfaces are also observed within channelised barforms and these are typically inclined at moderate angles of 10° to 15° which show no consistent orientation.

Trace fossils including *Protichnites*, *Scolicia* and *Thalassinoides* are common and are especially evident on the surfaces of finer-grained beds within fossiliferous grainstone facies (M3; table 1) at the top of this element. Individual sets within this element are typically 2 to 3 m and are characterised internally by poorly-defined planar and trough cross-bedding that is notably evident in examples of this element that possess a channel-like geometry. Sets are grouped into 8 m-thick cosets, within which each set is bounded by an erosional bounding surface.

Interpretation. This element represents the migration of subaqueous barforms in a shallow-marine or marginal marine setting (Dalrymple and Rhodes, 1995; Dalrymple and Choi, 2007). Variations in geometry between layered tabular sheets and laterally- and vertically-stacked channelised elements arise as a function of their position relative to the margins of the incised valley systems (discussed below). The bounding surfaces compartmentalising crossbeds of differing scales are superimposition surfaces; recording the migration of smaller barforms over the flanks of larger (Allen, 1991). Inclined surfaces contained within individual sets that truncate crossbeds are interpreted as reactivation surfaces (McCabe and Jones, 1977). The presence of broken shelly fauna and the coarse-grained nature of the siliciclastic material denote accumulation in a relatively high-energy setting, possibly marginal to the coastline, where fluvial systems were able to contribute significant volumes of siliciclastic detritus. Sigmoidal inclined surfaces seen in the channelised barforms are interpreted as inclined heterolithic stratification (*sensu* Thomas et al., 1987).

The presence of reactivation surfaces, compound barform migration and inclined heterolithic stratification are interpreted as the product of deposition within an estuarine environment (Boyd et al., 1992).

5 Geometry and Architecture of Incised Valley Systems

Three separate, time-independent incised valley systems are recognised with the architectural panel data set (figures 10 to 12), which collectively depicts the stratigraphy of the upper 70 m of the lower Cutler beds in the Shafer Basin and Indian Creek field localities. A series of allogenic controls have been shown to have operated through the duration represented by the accumulation of the low Cutler beds and these processes exerted a dominant control on the creation and subsequent fill of the incised valley systems (Rankey, 1997; Jordan, 2006; Jordan and Mountney, 2010; 2012). Indeed, numerous other incised valley systems have been noted (though not studied in detail) in the underlying 90 to 100 m of the formation (Huntoon et al., 1982). Of the three incised valley systems considered in detail as part of this study, the stratigraphically youngest (associated with flooding surface 12; FS12 of Jordan and Mountney, 2012) is characterized in figure 12, whereas the two remaining older incised valley systems are identified and characterized in all architectural panels data sets (figures 10 to 12).

The lower bounding surfaces of the incised valley systems are identified on the basis of the presence of erosive surfaces of regional lateral extent. These surfaces are usually overlain by fluvial channel or overbank elements or, where these types are absent, by channelised granulestone barform elements. The lateral margins of the incised valley systems are identified by an abrupt lateral transition from non-marine to marine elements types, most typically channelised granulestone barform elements. These marine-influenced elements only occur within the confines of the incised valley systems, their morphology and geometry being directly related to their location within a relatively confined topographic valley system. As such, their presence is the most reliable indicator of a setting within an incised valley system. Architectural elements associated with stratal surfaces that define the top of the incised valley systems include tabular sheet-like granulestone barform elements or, where these are absent, limestone elements.

The gross-scale geometries of the incised valley complexes present in the lower Cutler beds can be difficult to define since identification of their lateral bounding surfaces is not straightforward. The incised valleys studied in detail are each 8 to 12 m thick, though examples in more basinward locations (to the southwest) attain thicknesses of over 20 m (Jordan and Mountney, 2012). The widths of individual valley systems in orientations perpendicular to regional fluvial flow direction (NW-SE) are poorly constrained due to lack of continuity of outcrop but individual studied examples are each in excess of 1 km, which defines a minimum width. Although difficult to determine, the downstream length over which

individual incised valley systems can be traced is at least 40 km based on a well exposed example that can be traced from Indian Creek to Little Spring Canyon (figure 13).

Downstream (basinward) locations within the incised valley systems, which are exposed further to the southwest typically lack the basal fill by fluvial elements that are common in upstream settings (compare figure 11 and 13). The basal fill of valley systems in such locations is dominated by elements of shallow-marine origin, including granulestone barform elements. By contrast, a progressive replacement of shallow-marine deposits by fluvial deposits is noted in localities lying further to the northeast. Furthermore, within basinward settings, where shallow-marine accumulation dominated, the thickness and continuity of channelised granulestone barforms is greater, reflecting a significant shallow-marine influence. Regardless of location, the upper parts of the incised valley fills are dominated by granulestone barform elements, signifying the progressive transgression of a marine shoreline to a more proximal during episodes of relative sea-level rise.

The most landward limit of the studied incised valley systems is situated in the Shafer Basin locality (figure 3). Here, elements of shallow-marine origin are confined to the upper parts of the valley infills, whereas fluvial elements dominate in the middle and lower parts of the infill. This volumetric reduction in the incidence of preserved shallow-marine element types is due chiefly to a reduction in the occurrence of granulestone barform elements (figure 12). Present granulestone barforms are almost entirely characterised by sheet-like geometries, differing markedly from other field locations. Channelised granulestone barform elements are notably thinner in such instances; commonly less than 4 m than in more seaward areas, where they are typically 5 to 10 m thick. In the Shafer Basin, the preservation of a thicker unit of shallow-marine origin toward the top of the succession (~51 m up from base of panel, figure 12) records a compound succession of laterally and vertically stacked channelised and sheet-like granulestone barforms. By contrast, the fluvial succession in the middle part the succession (~35 m upwards from base of panel, figure 12) is preserved directly above an erosive surface. This succession, however, has no shallow-marine elements that would normally be expected during either back-filling within the valley system or transgression over the interfluvial areas. It is therefore interpreted that this relatively large (up to 13 m thick) succession of fluvial elements represents a location beyond the limit of the shoreline during highstand conditions for that specific relative sea-level cycle. Similarly, the small (1 to 3 m thick) succession of shallow-marine elements at the very top of the panel (figure 12) lacks the channelised granulestone elements that define deposition within the incised valley system. The preserved shallow-marine succession more readily matches the condensed shallow-marine successions that occurred on the interfluvial areas outside of the valley system (Jordan, 2006). Thus, the continued lack of defining characteristics of deposition

Version: Final draft**Updated:** 18/04/2013 12:13:45

completely within the incised valley system suggest that the Shafer Basin locality, though variable between cycles, occurs between a location beyond the highstand shoreline and the extreme landward end during most of the formation of the incised valley systems. Variation in the location relative to the incised valley system is apparently concordant with assertions by Jordan and Mountney (2012) where repeated relative sea-level cycles appear to be superimposed upon a larger-scale rising trend of relative sea-level.

Within each incised valley fill, several types of significant stratal surface are identified, each representing an important component of the development of the valley system in response to its evolution from lowstand to highstand as the valley systems became infilled. Identification of these stratigraphic surfaces and assignment of a genetic significance has been undertaken using the following criteria: (i) a vertical change from one depositional environment to another (e.g. fluvial to aeolian); (ii) a sharp lateral change from one depositional environment to another, reflecting a transition from deposition within to beyond the confines of the valley system. Using these criteria, two different types of stratigraphic surfaces have been identified associated with development of the incised valley systems and their infills (figures 10 to 12). The first of these are erosional surfaces that mark the lower and lateral margin bounding surfaces of the incised valley systems, predominately denoted by the presence of aeolian elements that are erosively overlain by fluvial channel and overbank elements (bold green lines on figures 10 to 12). Secondly transgressive surfaces that record the onset of shallow-marine processes that drowned interfluvial areas (Shanley and McCabe, 1993); these are usually marked by a change in depositional style between channelised and sheet-like granulestone barforms (bold red lines; figure 10 to 12). The timing of generation of these stratigraphic surfaces is considered later in the discussion section.

The incised valley systems and their styles of infill are comparable to several similar examples described from other studies whereby their style of infill records a predictable succession (Allen and Posamentier, 1993; Archer et al., 1994; Ashley et al., 1994; Dalrymple et al., 1994; Schumm and Ethridge, 1994; Posamentier, 2001; Green, 2009; Chaumillon et al., 2010). The infill typically composed of a lowermost basal fluvial unit (fluvial channel elements) that exhibits an upward transition into an overlying estuarine unit that marks the back-flooding of the incised valley system (channelised granulestone barforms). This culminates in an upward transition into a unit indicative of open (unconfined) marine conditions (sheet-like granulestone barforms and marine limestone elements; figures 11 and 12). Within some of the incised valley infills variations on this trend are evident, reflecting relatively more proximal (landward) and distal (basinward) positions within the incised valley systems, with landward and seaward settings experiencing more dominant fluvial and

shallow-marine styles of sedimentation, respectively (Li et al., 2002; Green, 2009; Cooper et al., 2012).

The similarities in the recorded signatures within incised valley systems of the lower Cutler beds are unlikely to have occurred solely from fluvial scour arising from fluvial channel avulsion for the following reasons: (i) the style of preserved infill follows that expected for incised valley systems and also exhibits upstream and downstream variation (Plink-Björklund, 2008); and (ii) the required driving mechanisms responsible for creating non-tectonically induced incised valley systems (i.e. relative sea-level cyclicity) have been identified by numerous authors across many basins of late Pennsylvanian to Permian age in the western United States (Dickinson et al., 1994; Goldhammer et al., 1994; Rankey, 1997; Jagger, 2003; Jordan, 2006; Mountney, 2006b; Cain, 2009).

6 Discussion

High-frequency relative sea-level changes responsible for moderating the accumulation of the lower Cutler beds have been previously attributed to so-called ~413 kyr eccentricity orbital cycles (Dickinson et al., 1994; Jordan and Mountney, 2010). In total, 12 marine transgressive-regressive cycles (sequences) are identified in the accessible part of the lower Cutler beds (Jordan and Mountney, 2010; 2012), with preservation of successive sequences having been enabled by the superimposition of relative sea-level cycles on a long-term subsidence trend responsible for generating accommodation (Nuccio and Condon, 1996). A depositional model that accounts for the origin of the observed stratigraphic architecture in response to one complete cycle of relative sea-level is presented here to account for the origin of the incised valley systems, and their subsequent fill by fluvial and shallow-marine strata (figure 14).

6.1 Highstand systems tract 1

During episodes of relative sea-level highstand, which equate to relatively more humid climatic conditions, the aeolian system underwent deconstruction under the influence of a deflationary wind regime, with significant portions of the land surface stabilised by vegetation and/or a high water table (Jordan, 2006). Increased fluvial discharge onto the coastal plain resulted in fluvial systems becoming dominant in inland areas (figures 10 to 12) and an increase in the volume of sediment being transported to and deposited within the alluvial coastal plain realm. The palaeo-shoreline occupied a landward position within the basin, the inland limit of transgression being demonstrated by the widespread occurrence of thin but regionally extensive tabular limestone units associated with the Maximum Flood Surface that defined the base of the highstand system tract (figure 12 and 14a).

6.2 Early falling-stage systems tract

Falling base-level associated with a lowering of relative sea-level resulted in a local increase in the gradient of the fluvial profile and initiated downcutting and incision by the fluvial systems (Shanley and McCabe, 1993; Koss et al., 1994). Incision would have resulted in the generation of an upstream-migrating knick-point, originating at the river mouth (Posamentier, 2001), especially where incision cut down through thin limestone horizons that were relatively resistant to erosion. This contrasts with other systems where contemporaneous incision along the entire length of the fluvial system has been proposed in response to regional tectonic uplift (Posamentier, 2001). Upstream knick-point migration significantly reduces channel mobility (Schumm, 1993; Ethridge et al., 1998) and, as such, the preservation potential of sediments deposited previously in overbank and interfluvial areas would likely have increased significantly (cf. Wright and Marriott, 1993). Deposition across more landward parts of the basin plain remained dominated by unconfined fluvial processes, as demonstrated by the occurrence of channel elements and extensive overbank elements arranged into wide belts (in excess of 400 m; figure 10). Fluvial incision in response to falling base-level initiated development of the incised valley systems (figure 14b). Incision along the fluvial system indicates that the amount of relative sea-level fall was sufficient for an incised valley system to form instead of a lowstand bypass channel (Posamentier, 2001). This type of incision most readily occurs in response to exposure of a shelf edge and an associated increase in the gradient of the fluvial profile (Posamentier, 2001; 2002). However, limestone elements within the lower Cutler beds have been interpreted previously to represent a ramp setting that lacked a distinct shelf-edge break in slope (Jordan, 2006; Jordan and Mountney, 2010). This suggests that the marine ramp that was present was likely inclined more steeply than the landward coastal plain (cf. Posamentier and Allen, 1999; Posamentier, 2001). Aeolian dune-field construction and accumulation likely commenced as increasingly arid climatic conditions developed as the lowstand was approached (see Jordan and Mountney, 2010, 2012). Coastline regression exposed extensive flat lying sandy coastal plain, which likely served as a potential sediment supply for aeolian system construction, with some potentially occurring as a lagged supply (Kocurek and Lancaster, 1999).

6.3 Late falling-stage systems tract

During the end of the falling-stage conditions, incision by fluvial channels progressed further upstream (Ethridge et al., 1998; Blum and Törnqvist, 2000). As incision occurred at a given location in the fluvial channel network, valley widening would have commenced (Leeder and Stewart, 1996). Valley widening would have initially enabled development of minor, gravity-driven slope instabilities; a consequence of oversteepening of the channel walls in response to lateral incision from the fluvial channel element (Schumm and Ethridge, 1994; Leeder and

Version: Final draft**Updated:** 18/04/2013 12:13:45

Stewart, 1996). These processes would have been exacerbated by low-frequency but relatively high-magnitude rainfall events (typical of fluvial floods in dryland systems) which would have promoted wall-collapse and incised valley growth via the enlargement of wadi systems (cf. Leeder and Stewart, 1996; Osterkamp and Friedman, 2000). As the channels incised further, so these processes became more prevalent, with downstream fluvial regions experiencing more lateral widening for two main reasons. Firstly, catchment area and discharge to incised valley systems tends to increase downstream, (Tuttle et al., 1966; Allen and Posamentier, 1993; Schumm and Ethridge, 1994); and secondly, downstream areas are the first to respond to incision in response to relative sea-level fall and it is suggested that this incision generated the steep valley walls required for the widening processes to operate (figure 14c; 15).

6.4 Lowstand systems tract

The vertical incision that formed the incised valley system would have ceased as the base-level stabilized (Dalrymple et al., 1994; figure 14d). Fluvial elements accumulated as the initial valley-fill in response to re-equilibration of the graded fluvial profile (figures 10 to 12), though the longer-term perseveration potential of these units varies (discussed below). An initially slow but progressive increase in relative sea-level resulted in shallow-marine flooding within incised valley mouths and led to deposition of mixed fluvial and shallow-marine facies types (F1, F2, F7, M2, M3 and M4; table 1) indicative of estuarine conditions (figures 10 to 12). This interplay between the fluvial and shallow-marine systems likely formed small bayhead deltas similar to those proposed by Terrell (1972) and synonymous with comparable modern examples (Dabrio et al., 2000; Heap et al., 2004).

Shallow-marine elements initially accumulated as part of the incised valley infills (figures 10 to 11), representing back-flooding of the incised valley system by shallow-marine waters. The infill of most of the incised valley systems exhibits an upward transition from fluvial facies to progressively more shallow-marine dominated facies (figures 10 to 12). This style of infill demonstrates a position within an incised valley system located seaward of the eventual highstand shoreline position. By contrast some valley-fill examples in the Shafer Basin representative of more landward settings (figure 12) lack shallow-marine elements reflecting a location beyond the limits of the highstand shoreline position (Posamentier and Allen, 1999; Posamentier, 2001). Such examples record minor incision driven by relatively modest changes in base-level, essentially differing from the marine-influenced incised valley systems located more basinward (Archer et al., 1994). Alternatively, changes in the rate and volume of fluvial discharge could also lead to the formation of minor incised valleys in

relatively landward settings, without the requirement for base-level variation (Cooper et al., 2012).

6.5 Late lowstand systems tracts

During the late lowstand system tract, the rate of relative sea-level rise began to accelerate and further back-flooding occurred within the marine-influenced incised valley systems. This culminated in the upper parts of the incised valleys becoming filled with facies indicative of open-marine conditions (figure 14e; Shanley and McCabe, 1993).

The lack of expected fluvial facies types within some of the basal parts of the incised valley differs somewhat from the idealised incised valley-fill models (cf. Dalrymple et al., 1994; Zaitlin et al., 1994; Posamentier, 2001); the absence of these fluvial elements possibly records a lack of preservation (figures 10 to 12), possibly as a result of transgressive scour during back-flooding of the valley by marine waters where the rate of transgression was sufficiently slow to enable protracted time for erosion and re-working of earlier fluvial deposits, perhaps by wave or tidal processes. Given the relatively large grain-sizes associated with constituent facies of the granulestone barform element (table 1), energy conditions were sufficiently high to locally rework earlier fluvial accumulations (figure 14f). Where the basal fluvial elements are locally absent (figures 10 to 12) shallow-marine elements directly overlie aeolian sand dune elements, the boundary between the two marking a significant bounding surface that defines the base of the incised valley system. In such examples the stratigraphically older aeolian sand dune elements represent units deposited beyond the confines of the incised valley system.

6.6 Transgressive systems tract

The change in depositional style within granulestone barforms from channelised to sheet-like elements records a switch in accumulation from within to beyond the confines of the incised valley system. Laterally more extensive, thinner, finer-grained and tabular sheet-like granulestone barform elements record deposition outside of the incised valley systems, where the lack of confinement by the valley walls reduced the energy regime of the depositional setting considerably. Conversely the channelised forms of this element occur as a result of the higher energy regimes resulting from direct confinement of shallow-marine waters within incised valley systems. This change in style marks the flooding of the interfluvial areas (transgressive surface), which in turn marks the onset of the transgressive system tract, with the base of laterally extensive sheet-like granulestone elements representing the initial flooding surface across the older interfluvial. Where sheet-like granulestone barforms are absent, the base of limestone elements is interpreted as representing this flooding surface.

Drowning of the incised valley system occurred during transgression with the valley system containing a thicker and more complete preserved record of relative sea-level fluctuations compared to the adjacent areas outside of the valley system (interfluves), which generally record a condensed succession.

6.7 Highstand systems tract

At highstand, marine transgression reached its furthest position inland; with marine waters flooding extensive areas of the coastal plain (figure 14g). Limestone elements indicative of open marine conditions, which began accumulating during transgression, became more dominant during highstand conditions. The uppermost limestone elements that tend to define highstand system tracts generally being the uppermost elements present in preserved sequences (Jordan and Mountney, 2012), and the limestone element at the top of the succession recording the uppermost unit in the lower Cutler beds (figures 10 to 12). This limestone unit is highly continuous over a lateral extent of several thousand km², and is therefore too extensive to be the product of accumulation within the confines of the incised valley system.

Fluvial elements, passing upwards into successions of mixed fluvio-marine and finally into laterally continuous sediments of shallow-marine origin detail the style of infill and drowning of a single incised valley system. The types of valley fills record the product of a single cycle of base-level fall and rise and associated interdependent changes in climate, rather than multiple phases of cut and infill, as have been described for other systems with apparently similar geometries and styles of infill (Ashley et al., 1994; Dalrymple et al., 1994; Levy et al., 1994).

7 Conclusions

The lower Cutler beds represent the preserved accumulation of a tripartite system of coeval aeolian, fluvial and shallow-marine depositional systems that developed in a lower alluvial plain, shoreline and shallow-marine setting in the Paradox foreland basin. Changes in base-level related to relative sea-level variations driven by Milankovitch-style cyclicity caused fluvial systems to incise during episodes of falling relative sea-level. Incision events associated with separate sequences resulted in the generation of multiple time-independent incised valley systems during the accumulation of the lower Cutler beds (figures 10 to 12). Episodes of relative sea-level rise resulted in back-flooding of the incised valley systems and the accumulation of a succession of mixed shallow-marine and fluvial affinity, passing upward within the fill of each incised valley succession into strata indicative of open marine conditions. Each incised valley system records an episode of cut-and-fill during a single

Version: Final draft**Updated:** 18/04/2013 12:13:45

cycle of base-level fall and rise; individual valley fills do not preserve evidence of multiple cut-and-fill events. The absence of fluvial architectural elements as the basal-most fill of some of the studied incised valley systems differs from idealised valley-fill models; erosion associated with high-energy conditions during marine transgression into these valley systems was likely responsible for reworking such fluvial deposits. The confinement of shallow marine waters within flooded embayments resulted in the preservation of two types of granulestone barform and limestone element: (i) thick, channelised, laterally restricted, vertically amalgamated and overlapping elements; (ii) thin, sheet-like, laterally extensive elements. Granulestone barform elements occurring in channelized features within the incised valley systems accumulated during lowstand, whereas marine limestone elements indicative of open-marine conditions accumulated during highstand. Relative sea-level rises were sufficient to fill and drown the incised valley systems, with transgression across interfluvies manifest as regionally correlatable limestone elements, the uppermost of which records the top of the lower Cutler beds.

8 Acknowledgements

Funding for this research was produced by grant awards to the lead author by the British Sedimentological Research Group and the International Association of Sedimentologists. Areva, BHP Billiton, ConocoPhillips, Nexen, Saudi Aramco, Shell and Woodside are thanked for supporting this research through their sponsorship of the Fluvial & Eolian Research Group. Stephen Cain, Jo Venus and Michael Rippon are thanked for their help and assistance in the field. Edward Hough and Phil Richards are thanked for their constructive comments in helping produce this study.

9 References

- Allen, G.P., 1991. Sedimentary processes and facies in the Gironde estuary: a recent model for macrotidal estuarine systems. In: D.G. Smith, G.E. Reinson, B.A. Zaitlin, R.A. Rahmani (Eds.), *Clastic tidal sedimentology*. Canadian Society of Petroleum Geologists Memoir, pp. 29-40.
- Allen, G.P., Posamentier, H.W., 1993. Sequence stratigraphy and facies model of an incised valley fill; the Gironde Estuary, France. *Journal of Sedimentary Research*, 63(3): 378-391.
- Archer, A.W., Lanier, W.P., Feldman, H.R., 1994. Stratigraphy and depositional history within incised-paleovalley fills and related facies, Douglas Group (Missourian / Virgillian; Upper Carboniferous) of Kansas USA. In: R.W. Dalrymple, R. Boyd, B.A. Zaitlin (Eds.). *Incised-Valley Systems: Origin and Sedimentary Sequences*. SEPM, Special Publication, pp. 175-190.
- Ashley, G.M., Sheridan, R.E., Dalrymple, R.W., Boyd, R., Zaitlin, B.A., 1994. Depositional model for valley fills on a passive continental margin. *Society of Economic Paleontologists and Mineralogists - Special Publication*, 51: 285-285.
- Atchley, S.C., Loope, D.B., 1993. Low-Stand Aeolian Influence on Stratigraphic Completeness: Upper Member of the Hermosa Formation (Latest Carboniferous), Southeast Utah, USA. In: K. Pye, N. Lancaster (Eds.), *Aeolian Sediments: Ancient and Modern*. International Association of Sedimentologists, Special Publication, pp. 127-149.
- Baars, D.L., 1962. Permian system of Colorado Plateau. *AAPG Bulletin*, 46(2): 149-218.
- Baars, D.L., 1979. The Permian System. In: D.L. Baars (Ed.), *Permianland*. Four Corners Geological Society, Durango, CO, 9th Field Conference Guidebook.
- Barbeau, D.L., 2003. A flexural model for the Paradox Basin: implications for the tectonics of the Ancestral Rocky Mountains. *Basin Research*, 15(1): 97-115.
- Blakey, R.C., 2008. Pennsylvanian–Jurassic sedimentary basins of the Colorado Plateau and southern Rocky Mountains. In: A.D. Miall (Ed.), *Sedimentary Basins of the United States and Canada*. Elsevier, Amsterdam, pp. 245-296.
- Blakey, R.C., 2009. Paleogeography and Geologic History of the western Ancestral Rocky Mountains, Pennsylvanian-Permian, Southern Rocky Mountains and Colorado Plateau. In: B. Houston, P. Moreland, L. Wray (Eds.). *The Paradox Basin: Recent Advancements in Hydrocarbon Exploration*. Rocky Mountain Association of Geologists Special Publication, pp. 222-264.
- Blakey, R.C., Havholm, K.G., Jones, L.S., 1996. Stratigraphic analysis of eolian interactions with marine and fluvial deposits, Middle Jurassic Page Sandstone and Carmel Formation, Colorado Plateau, USA. *Journal of Sedimentary Research*, 66(2): 324-342.
- Blakey, R.C., Knepp, R., 1989. Pennsylvanian and Permian geology of Arizona. In: J.P. Jenney, S.J. Reynolds (Eds.), *Geologic Evolution of Arizona: Arizona Geological Society, Digest*, pp. 313-347.
- Blum, M.D., Törnqvist, T.E., 2000. Fluvial responses to climate and sea-level change: a review and look forward. *Sedimentology*, 47: 2-48.
- Boyd, R., Dalrymple, R., Zaitlin, B.A., 1992. Classification of clastic coastal depositional environments. *Sedimentary Geology*, 80(3–4): 139-150.
- Bullard, J.E., Livingstone, I., 2002. Interactions between aeolian and fluvial systems in dryland environments. *Area*, 34(1): 8-16.
- Cain, S.A., 2009. Sedimentology and stratigraphy of a terminal fluvial fan system: the Permian Organ Rock Formation, South East Utah. unpublished Thesis, Keele University.
- Campbell, J.A., 1980. Lower Permian depositional systems and Wolfcampian paleogeography, Uncompahgre basin, eastern Utah and southwestern Colorado. In: T.D. Fouch, E.R. Magathan (Eds.), *Paleozoic Paleogeography of West-Central United States*, SEPM, Rocky Mountain Section, pp. 327-340.
- Chaumillon, E., Tessier, B., Reynaud, J.-Y., 2010. Stratigraphic records and variability of incised valleys and estuaries along French coasts. *Bulletin de la Societe Geologique de France*, 181(2): 75-85.

Version: Final draft**Updated:** 18/04/2013 12:13:45

- Condon, S.M., 1997. Geology of the Pennsylvanian and Permian cutler group and Permian Kaibab limestone in the Paradox Basin, southeastern Utah and southwestern Colorado. US Government Printing Office.
- Cooper, J.A.G., Green, A.N., Wright, C.I., 2012. Evolution of an incised valley coastal plain estuary under low sediment supply: a 'give-up' estuary. *Sedimentology*, 59(3): 899-916.
- Dabrio, C.J. et al., 2000. Depositional history of estuarine infill during the last postglacial transgression (Gulf of Cadiz, Southern Spain). *Marine Geology*, 162(2-4): 381-404.
- Dalrymple, R.W., Boyd, R., Zaitlin, B.A., 1994. History of research, types and internal organization of incised-valley systems: Introduction to the volume. In: R.W. Dalrymple, R. Boyd, B.A. Zaitlin (Eds.). *Incised-Valley Systems: Origin and Sedimentary Sequences*. SEPM, Special Publication, pp. 3-10.
- Dalrymple, R.W., Choi, K., 2007. Morphologic and facies trends through the fluvial-marine transition in tide-dominated depositional systems: A schematic framework for environmental and sequence-stratigraphic interpretation. *Earth-Science Reviews*, 81(3-4): 135-174.
- Dalrymple, R.W., Rhodes, R.N., 1995. Estuarine Dunes and Bars. In: P.G.M. E. (Ed.), *Developments in sedimentology*. Elsevier, pp. 359-422.
- Dickinson, W.R., Soreghan, G.S., Giles, K.A., 1994. Glacio-eustatic origin of Permo-Carboniferous stratigraphic cycles: Evidence from the southern Cordilleran foreland region. In: J.M. Dennison, F.R. Etensohn (Eds.), *Tectonic and eustatic controls on sedimentary cycles*. SEPM Concepts in Sedimentology and Paleontology, pp. 25-34.
- Doe, T.W., Dott Jr, R.H., 1980. Genetic Significance of Deformed Cross Bedding--With Examples from the Navajo and Weber Sandstones of Utah. *Journal of Sedimentary Research*, 50(3).
- Ethridge, F.G., Wood, L.J., Schumm, S., 1998. Cyclic variables controlling fluvial sequence development: problems and perspectives. In: K.W. Shanley, P.J. McCabe (Eds.). *Relative role of Eustasy, Climate and Tectonism on Continental Rocks*. SEPM Special Publication, pp. 17-29.
- Goldhammer, R.K., Oswald, E.J., Dunn, P.A., 1994. High-Frequency, Glacio-Eustatic Cyclicity in the Middle Pennsylvanian of the Paradox Basin: An Evaluation of Milankovitch Forcing. In: P.L. Boer, D.G. Smith (Eds.). *Orbital Forcing and Cyclic Sequences*. International Association of Sedimentologists, Special Publication, pp. 243-283.
- Green, A.N., 2009. Palaeo-drainage, incised valley fills and transgressive systems tract sedimentation of the northern KwaZulu-Natal continental shelf, South Africa, SW Indian Ocean. *Marine Geology*, 263(1-4): 46-63.
- Heap, A.D., Bryce, S., Ryan, D.A., 2004. Facies evolution of Holocene estuaries and deltas: a large-sample statistical study from Australia. *Sedimentary Geology*, 168(1-2): 1-17.
- Heckel, P.H., 1980. Paleogeography of eustatic model for deposition of Midcontinent Upper Pennsylvanian cyclothems. In: T.D. Fouch, E.R. Magathan (Eds.), *Society of Economic Paleontologists and Mineralogists, Rocky Mountain Section. Paleozoic Paleogeography of West-Central United States* pp. 197-215.
- Horowitz, D.H., 1982. Geometry and origin of large-scale deformation structures in some ancient wind-blown sand deposits. *Sedimentology*, 29(2): 155-180.
- Hunter, R.E., 1977. Basic types of stratification in small eolian dunes. *Sedimentology*, 24(3): 361-387.
- Hunter, R.E., 1981. Stratification styles in eolian sandstones: some Pennsylvanian to Jurassic examples from the Western Interior U.S.A. In: F.G. Ethridge, R.M. Flores (Eds.), *Recent and Ancient Nonmarine Depositional Environments: Models for Exploration*. Society for Economic Paleontologists and Mineralogists, pp. 315-329.
- Huntoon, P.W., Billingsley, G.H., J., B.W., 1982. Geologic Map of Canyonlands National Park and vicinity, Utah. Canyonlands Natural History Association Moab, Utah
- Jagger, A., 2003. Sedimentology and Stratigraphic evolution of the Permian Cedar Mesa sandstone, Paradox Basin, SE Utah. unpublished Thesis, Keele University.

Version: Final draft**Updated:** 18/04/2013 12:13:45

- Jordan, O.D., 2006. Sedimentology and stratigraphic evolution of the Pennsylvanian-Permian Lower Cutler Beds, Paradox basin, SE Utah. unpublished Thesis, Keele University.
- Jordan, O.D., Mountney, N.P., 2010. Styles of interaction between aeolian, fluvial and shallow marine environments in the Pennsylvanian to Permian lower Cutler beds, south-east Utah, USA. *Sedimentology*, 57(5): 1357-1385.
- Jordan, O.D., Mountney, N.P., 2012. Sequence Stratigraphic Evolution and Cyclicity of An Ancient Coastal Desert System: The Pennsylvanian-Permian Lower Cutler Beds, Paradox Basin, Utah, U.S.A. *Journal of Sedimentary Research*, 82(10): 755-780.
- Kluth, C.F., Duchene, H.R., 2009. Late Pennsylvanian and Early Permian structural geology and tectonic history of the Paradox Basin and Uncompahgre Uplift, Colorado and Utah. In: W.S. Houston, L.L. Wray, P.G. Moreland (Eds.). *The Paradox Basin Revisited—New Developments in Petroleum Systems and Basin Analysis*. Rocky Mountain Association of Geologists Special Publication, pp. 178-197.
- Kocurek, G., 1981. ERG reconstruction: The entrada sandstone (Jurassic) of northern Utah and Colorado. *Palaeogeography, Palaeoclimatology, Palaeoecology*, 36(1-2): 125-153.
- Kocurek, G., 1999. The aeolian rock record (Yes, Virginia, it exists, but it really is rather special to create one). In: A.S. Goudie, I. Livingstone, S. Stokes (Eds.). *Aeolian Environments, Sediments and Landforms*. Wiley, New York, pp. 259.
- Kocurek, G., Lancaster, N., 1999. Aeolian system sediment state: theory and Mojave Desert Kelso dune field example. *Sedimentology*, 46(3): 505-515.
- Koss, J.E., Ethridge, F.G., Schumm, S., 1994. An experimental study of the effects of base-level change on fluvial, coastal plain and shelf systems. *Journal of Sedimentary Research*, 64(2): 90-98.
- Krapf, C.B.E., Stollhofen, H., Stanistreet, I.G., 2003. Contrasting styles of ephemeral river systems and their interaction with dunes of the Skeleton Coast erg (Namibia). *Quaternary International*, 104(1): 41-52.
- Kunkel, R.P., 1958. Permian stratigraphy of the Paradox basin. In: A.F. Sanborn (Ed.). *Guidebook to the Geology of the Paradox Basin Intermontaine Association of Petroleum Geologists*, Salt Lake City, Utah, pp. 163-168.
- Lancaster, N., 1983. Controls of Dune Morphology in the Namib Sand Sea. In: B.M. E., A.T. S. (Eds.), *Developments in Sedimentology*. Elsevier, pp. 261-289.
- Langford, R.P., 1989. Fluvial-aeolian interactions: Part I, modern systems. *Sedimentology*, 36(6): 1023-1035.
- Langford, R.P., Chan, M.A., 1988. Flood surfaces and deflation surfaces within the Cutler Formation and Cedar Mesa Sandstone (Permian), southeastern Utah. *Geological Society of America Bulletin*, 100(10): 1541-1549.
- Langford, R.P., Chan, M.A., 1989. Fluvial-aeolian interactions: Part II, ancient systems. *Sedimentology*, 36(6): 1037-1051.
- Langford, R.P., Chan, M.A., 1993. Downwind Changes within an Ancient Dune Sea, Permian Cedar Mesa Sandstone, Southeast Utah. In: K. Pye, N. Lancaster (Eds.). *Aeolian Sediments: Ancient and Modern*. International Association of Sedimentologists, Special Publication, pp. 109-126.
- Leeder, M.R., Stewart, M.D., 1996. Fluvial incision and sequence stratigraphy: alluvial responses to relative sea-level fall and their detection in the geological record. *Geological Society, London, Special Publications*, 103(1): 25-39.
- Levy, M., Christie-Blick, N., Link, P.K., 1994. Neoproterozoic incised valleys of the eastern Great Basin, Utah and Idaho: Fluvial response to changes in depositional base level. In: R.W. Dalrymple, R. Boyd, B.A. Zaitlin (Eds.). *Incised-Valley Systems: Origin and Sedimentary Sequences*. SEPM, Special Publication, pp. 369-369.
- Li, C. et al., 2002. Late Quaternary incised-valley fill of the Yangtze delta (China): its stratigraphic framework and evolution. *Sedimentary Geology*, 152(1-2): 133-158.

Version: Final draft**Updated:** 18/04/2013 12:13:45

- Loope, D.B., 1981. Deposition, deflation and diagenesis of Upper Paleozoic eolian sediments, Canyonlands National Park, Utah. unpublished Thesis, University of Wyoming, Laramie.
- Loope, D.B., 1984. Eolian Origin of Upper Paleozoic Sandstones, Southeastern Utah. *Journal of Sedimentary Research*, 54(2): 563-580.
- Loope, D.B., 1985. Episodic deposition and preservation of eolian sands: A late Paleozoic example from southeastern Utah. *Geology*, 13(1): 73-76.
- Loope, D.B., 1988. Rhizoliths in ancient eolianites. *Sedimentary Geology*, 56(1-4): 301-314.
- Loope, D.B., Sanderson, G.A., Verville, G.J., 1990. Abandonment of the name Elephant Canyon Formation in southeastern Utah: Physical and temporal implications. *Mountain Geologist*, 27(4): 119-130.
- Mack, G.H., 1977. Depositional environments of the Cutler-Cedar Mesa facies transition (Permian) near Moab, Utah. *Mountain Geologist*, 14: 53-68.
- Mack, G.H., 1978. The survivability of labile light-mineral grains in fluvial, aeolian and littoral marine environments: the Permian Cutler and Cedar Mesa Formations, Moab, Utah. *Sedimentology*, 25(5): 587-604.
- Mack, G.H., Rasmussen, K.A., 1984. Alluvial-fan sedimentation of the Cutler Formation (Permo-Pennsylvanian) near Gateway, Colorado. *Geological Society of America Bulletin*, 95(1): 109-116.
- McCabe, P.J., Jones, C.M., 1977. Formation of Reactivation Surfaces Within Superimposed Deltas and Bedforms. *Journal of Sedimentary Research*, 47(2): 707-715.
- McKnight, E.T., 1940. Geology of area between Green and Colorado rivers, Grand and San Juan counties, Utah. *US Geological Survey Bulletin*, 908: 147.
- Mountney, N.P., 2006a. Eolian facies models. In: H.W. Posamentier, R.G. Walker (Eds.). *Facies Models Revisited*. Society of Economic Paleontologists and Mineralogists Memoir, pp. 19-83.
- Mountney, N.P., 2006b. Periodic accumulation and destruction of aeolian erg sequences in the Permian Cedar Mesa Sandstone, White Canyon, southern Utah, USA. *Sedimentology*, 53(4): 789-823.
- Mountney, N.P., 2012. A stratigraphic model to account for complexity in aeolian dune and interdune successions. *Sedimentology*, 59(3): 964-989.
- Mountney, N.P., Jagger, A., 2004. Stratigraphic evolution of an aeolian erg margin system: the Permian Cedar Mesa Sandstone, SE Utah, USA. *Sedimentology*, 51(4): 713-743.
- Mountney, N.P., Thompson, D.B., 2002. Stratigraphic evolution and preservation of aeolian dune and damp/wet interdune strata: an example from the Triassic Helsby Sandstone Formation, Cheshire Basin, UK. *Sedimentology*, 49(4): 805-833.
- Nuccio, V.F., Condon, S.M., 1996. Burial and thermal history of the Paradox Basin, Utah and Colorado, and petroleum potential of the middle Pennsylvanian Paradox Formation. *US Geological Survey Bulletin*.
- Osterkamp, W.R., Friedman, J.M., 2000. The disparity between extreme rainfall events and rare floods – with emphasis on the semi-arid American West. *Hydrological Processes*, 14: 2817-2829.
- Plink-Björklund, P., 2008. Wave-to-Tide Process Change in a Campanian Shoreline Complex, Chimney Rock Tongue, Wyoming and Utah. In: G.J. Hampson, R.J. Steel, P.M. Burgess, R.W. Dalrymple (Eds.), *Recent advances in Models of Siliciclastic Shallow-Marine Stratigraphy* SEPM Special Publication, pp. 265-291.
- Posamentier, H.W., 2001. Lowstand Alluvial Bypass Systems: Incised vs. Unincised. *AAPG Bulletin*, 85(10): 1771-1793.
- Posamentier, H.W., 2002. Ancient Shelf Ridges—A Potentially Significant Component of the Transgressive Systems Tract: Case Study from Offshore Northwest Java. *AAPG Bulletin*, 86(1): 75-106.
- Posamentier, H.W., Allen, G.P., 1999. *Siliciclastic Sequence Stratigraphy – Concepts and Applications*. SEPM Concepts in Sedimentology and Palaeontology, 7, 216 pp.

Version: Final draft**Updated:** 18/04/2013 12:13:45

- Rankey, E.C., 1997. Relations between relative changes in sea level and climate shifts: Pennsylvanian–Permian mixed carbonate-siliciclastic strata, western United States. *Geological Society of America Bulletin*, 109(9): 1089-1100.
- Rasmussen, L., Rasmussen, D.L., 2009. Burial History Analysis of the Pennsylvanian Petroleum System in the Deep Paradox Basin Fold and Fault Belt, Colorado and Utah. In: W.S. Houston, L.L. Wray, P.G. Moreland (Eds.). *The Paradox Basin Revisited—New Developments in Petroleum Systems and Basin Analysis*. Rocky Mountain Association of Geologists Special Publication, pp. 24-94.
- Rubin, D.M., 1987. Formation of scalloped cross-bedding without unsteady flows. *Journal of Sedimentary Research*, 57(1): 39-45.
- Rubin, D.M., Hunter, R.E., 1983. Reconstructing Bedform Assemblages from Compound Crossbedding. In: M.E. Brookfield, T.S. Ahlbrandt (Eds.). *Eolian Sediments and Processes*. Developments in Sedimentology, pp. 407-427.
- Schumm, S.A., 1993. River response to baselevel change: implications for sequence stratigraphy. *The Journal of Geology*, 101(2): 279-294.
- Schumm, S.A., Ethridge, F.G., 1994. Origin, evolution and morphology of fluvial valleys. In: R.W. Dalrymple, R. Boyd, B.A. Zaitlin (Eds.), SEPM, Special Publication. *Incised-Valley Systems: Origin and Sedimentary Sequences*, pp. 11-27.
- Shanley, K.W., McCabe, P.J., 1993. Alluvial Architecture in a Sequence Stratigraphic Framework: A Case History from the Upper Cretaceous of Southern Utah, USA. In: S.S. Flint, I.D. Bryant (Eds.), *The Geological Modelling of Hydrocarbon Reservoirs and Outcrop Analogues*. Quantitative Modelling of Clastic Hydrocarbon Reservoirs and Outcrop Analogs International Association of Sedimentologists, Special Publication, pp. 21-55.
- Simpson, E.L., Eriksson, K.A., 1993. Thin eolianites interbedded within a fluvial and marine succession: early proterozoic whitworth formation, mount isa inlier, australia. *Sedimentary Geology*, 87(1–2): 39-62.
- Soreghan, G.S., 1994. Stratigraphic responses to geologic processes: Late Pennsylvanian eustasy and tectonics in the Pedregosa and Orogrande basins, Ancestral Rocky Mountains. *Geological Society of America Bulletin*, 106(9): 1195-1211.
- Soreghan, G.S., Elmore, R.D., Lewchuk, M.T., 2002. Sedimentologic-magnetic record of western Pangean climate in upper Paleozoic loessite (lower Cutler beds, Utah). *Geological Society of America Bulletin*, 114(8): 1019-1035.
- Stanescio, J.D., Campbell, J.A., 1989. Eolian and noneolian facies of the lower Permian Cedar Mesa Sandstone Member of the Cutler Formation, southeastern Utah. *US Geological Survey Bulletin*, 1808-M: 13.
- Stanescio, J.D., Dubiel, R.F., Huntoon, J.E., 2000. Depositional environments and paleotectonics of the Organ Rock Formation of the Permian Cutler Group, southeastern Utah. In: D.A. Sprinkel, T.C. Chidsey, P.B. Anderson (Eds.), *Geology of Utah's National Parks and Monuments* Utah Geological Association Publication, pp. 591-605.
- Stanistreet, I.G., Stollhofen, H., 2002. Hoanib River flood deposits of Namib Desert interdunes as analogues for thin permeability barrier mudstone layers in aeolianite reservoirs. *Sedimentology*, 49(4): 719-736.
- Terrell, F.M., 1972. Lateral facies and paleoecology of Permian Elephant Canyon Formation, Grand County, Utah. *Brigham Young University Geology Studies*, 19: 3-44.
- Thomas, R.G. et al., 1987. Inclined heterolithic stratification - Terminology, description, interpretation and significance. *Sedimentary Geology*, 53(1–2): 123-179.
- Tooth, S., 1999. Floodouts in central Australia. In: A.J. Miller, A. Gupta (Eds.). *Varieties of fluvial form*. Wiley and Sons, London, pp. 219-247.
- Tooth, S., 2000. Downstream changes in dryland river channels: the Northern Plains of arid central Australia. *Geomorphology*, 34(1–2): 33-54.

Version: Final draft**Updated:** 18/04/2013 12:13:45

- Tooth, S., 2005. Splay Formation Along the Lower Reaches of Ephemeral Rivers on the Northern Plains of Arid Central Australia. *Journal of Sedimentary Research*, 75(4): 636-649.
- Trudgill, B.D., 2011. Evolution of salt structures in the northern Paradox Basin: controls on evaporite deposition, salt wall growth and supra-salt stratigraphic architecture. *Basin Research*, 23(2): 208-238.
- Tucker, M.E., Wright, V.P., 1990. *Carbonate Sedimentology*. Wiley-Blackwell, Cambridge.
- Tuttle, S.D., Milling, M.E., Rusnak, R.S., 1966. Comparisons of stream sizes (discharge) with valley sizes and shapes. *Geological Society of America, Special Paper*, 101: 225.
- Van Wagoner, J.C., Mitchum, R.M., Campion, K.M., Rahmanian, V.D., 1990. Siliciclastic Sequence Stratigraphy in Well Logs, Cores, and Outcrops: Concepts for High-Resolution Correlation of Time and Facies. *AAPG Methods In Exploration*, 7, 45 pp.
- Williams, M.R., 1996. Stratigraphy of Upper Pennsylvanian cyclical carbonate and siliciclastic rocks, western Paradox Basin. In: M.W. Longman, M.D. Sonnenfeld (Eds.). *Paleozoic Systems of the Rocky Mountain Region. Rocky Mountain Section – SEPM, Denver, CO.*, pp. 283-304.
- Wright, P.V., 1994. Paleosols in shallow marine carbonate sequences. *Earth-Science Reviews*, 35(4): 367-395.
- Wright, P.V., Marriott, S.B., 1993. The sequence stratigraphy of fluvial depositional systems: the role of floodplain sediment storage. *Sedimentary Geology*, 86(3–4): 203-210.
- Zaitlin, B.A., Dalrymple, R.W., Boyd, R., 1994. The stratigraphic organization of incised-valley systems associated with relative sea-level change. In: R.W. Dalrymple, R. Boyd, B.A. Zaitlin (Eds.). *Incised-Valley Systems: Origin and Sedimentary Sequences. SEPM, Special Publication*, pp. 45-60.

Figure and Table Captions

Table 1. Characteristics of common lithofacies present in the lower Cutler beds.

Figure 1. Summary stratigraphical chart for the Paradox Basin region.

Figure 2. Summary palaeogeography of the Paradox Basin during the Sakmarian (~290 Ma). Modified in part after Blakey (2008).

Figure 3. Field site location map (top-left) and individual location maps for the Indian Creek, Shafer Basin and Little Spring Canyon field localities. Darker grey colours depict areas of higher elevation in the field locality maps 1 - 3. Universal Transverse Mercator (UTM) co-ordinates shown.

Figure 4. Example lithofacies of the lower Cutler beds. (A) Erosively based set of facies M3 (base of sheet-like granulestone barform element), overlying facies M4 (upper portion of sheet-like granulestone barform element). (B) Interbeds of facies A1 and A3 (aeolian dune element). Reactivation surfaces evident; depicted by arrows. (C) Compound co-sets of facies F1 (fluvial channel element). Outcrop cuts near perpendicular to palaeoflow direction. (D) Facies M2 showing highly nodular appearance (marine limestone element). (E) Toesets of facies A1 interfingering with facies A2 (aeolian dune and interdune elements). (F) Facies F3 exhibiting horizontal lamination and near-horizontal lamination (overbank element). (G) Fine-grained sets of facies F4 (fluvial channel element). (H) Immature palaeosol facies (F5) with root nodules (overbank element).

Figure 4 (continued). Example lithofacies of the lower Cutler beds. (I) Facies F2 with both intra- and extra-formational clasts present (basal component of fluvial channel element). (J) Bedding surface of facies M1 exposing broken shelly fauna (limestone bench element). (K) Desiccation cracks and rain-drop imprints of facies F8 (damp interdune element). (L) Close-up of facies M3 detailing grain size variation (granulestone barform element). (M) Cross-bedded sets of facies M4 (granulestone barform element). (N) Highly contorted unit of facies F8 (damp interdune element). (O) Interbeds of facies F5, F6 and F7 (overbank and interdune elements). (P) Facies A1 and A3 overlying a thick succession of F7 (aeolian sand dune overlying fluvial channel element).

Figure 5. Model depicting the sedimentary architectural relationship between fluvial channel and aeolian sand dune elements.

Figure 6. Model depicting the sedimentary architectural relationship between aeolian sand dune and wet interdune elements.

Version: Final draft

Updated: 18/04/2013 12:13:45

Figure 7. Model depicting the sedimentary architectural relationship between fluvial channel and granulestone barform elements.

Figure 8. Model depicting the sedimentary architectural relationship between fluvial channel and fluvial overbank elements.

Figure 9. Model depicting the sedimentary architectural relationship between granulestone barform and limestone elements.

Figure 10. Architectural panel of lower Cutler beds at Indian Creek, Panel A. See Figure 3 for location.

Figure 11. Architectural panel of lower Cutler beds at Indian Creek, Panel B. See Figure 3 for location.

Figure 12. Architectural panel of lower Cutler beds at Shafer Basin. See Figure 3 for location.

Figure 13. Little Spring Canyon correlation panel. Log correlations depict individual architectural elements. See Figure 3 for location. Individual sedimentary log grainsize increases towards the right.

Figure 14a. Depositional and sequence stratigraphic model to account for the origin and style of infill of the incised valley systems present in the lower Cutler beds in response to combined relative sea-level and climatic change: Highstand systems tract 1. (A) highstand system tract; (B) falling-stage system tract; (C) late falling-stage system tract; (D) early low stand system tract; (E) middle lowstand system tract; (F) late lowstand system tract; (G) transgressive and highstand system tract. HST = Highstand Systems Tract, FSST = Falling-Stage Systems Tract, LST = Lowstand Systems Tract, TST = Transgressive Systems Tract.

Figure 14b. Depositional and sequence stratigraphic model to account for the origin and style of infill of the incised valley systems present in the lower Cutler beds in response to combined relative sea-level and climatic change: Falling-stage systems tract (A) highstand system tract; (B) falling-stage system tract; (C) late falling-stage system tract; (D) early low stand system tract; (E) middle lowstand system tract; (F) late lowstand system tract; (G) transgressive and highstand system tract. HST = Highstand Systems Tract, FSST = Falling-stage Systems Tract, LST = Lowstand Systems Tract, TST = Transgressive Systems Tract.

Figure 14c. Depositional and sequence stratigraphic model to account for the origin and style of infill of the incised valley systems present in the lower Cutler beds in response to

Version: Final draft**Updated:** 18/04/2013 12:13:45

combined relative sea-level and climatic change: Late falling-stage systems tract (A) highstand system tract; (B) falling-stage system tract; (C) late falling-stage system tract; (D) early low stand system tract; (E) middle lowstand system tract; (F) late lowstand system tract; (G) transgressive and highstand system tract. HST = Highstand Systems Tract, FSST = Falling-stage Systems Tract, LST = Lowstand Systems Tract, TST = Transgressive Systems Tract.

Figure 14d. Depositional and sequence stratigraphic model to account for the origin and style of infill of the incised valley systems present in the lower Cutler beds in response to combined relative sea-level and climatic change: Early lowstand systems tract. (A) highstand system tract; (B) falling-stage system tract; (C) late falling-stage system tract; (D) early low stand system tract; (E) middle lowstand system tract; (F) late lowstand system tract; (G) transgressive and highstand system tract. HST = Highstand Systems Tract, FSST = Falling-stage Systems Tract, LST = Lowstand Systems Tract, TST = Transgressive Systems Tract.

Figure 14e. Depositional and sequence stratigraphic model to account for the origin and style of infill of the incised valley systems present in the lower Cutler beds in response to combined relative sea-level and climatic change: Middle lowstand systems tract. (A) highstand system tract; (B) falling-stage system tract; (C) late falling-stage system tract; (D) early low stand system tract; (E) middle lowstand system tract; (F) late lowstand system tract; (G) transgressive and highstand system tract. HST = Highstand Systems Tract, FSST = Falling-stage Systems Tract, LST = Lowstand Systems Tract, TST = Transgressive Systems Tract.

Figure 14f. Depositional and sequence stratigraphic model to account for the origin and style of infill of the incised valley systems present in the lower Cutler beds in response to combined relative sea-level and climatic change: Late lowstand systems tract. (A) highstand system tract; (B) falling-stage system tract; (C) late falling-stage system tract; (D) early low stand system tract; (E) middle lowstand system tract; (F) late lowstand system tract; (G) transgressive and highstand system tract. HST = Highstand Systems Tract, FSST = Falling-stage Systems Tract, LST = Lowstand Systems Tract, TST = Transgressive Systems Tract.

Figure 14g. Depositional and sequence stratigraphic model to account for the origin and style of infill of the incised valley systems present in the lower Cutler beds in response to combined relative sea-level and climatic change: Highstand systems tract 2. (A) highstand system tract; (B) falling-stage system tract; (C) late falling-stage system tract; (D) early low stand system tract; (E) middle lowstand system tract; (F) late lowstand system tract; (G)

Version: Final draft

Updated: 18/04/2013 12:13:45

transgressive and highstand system tract. HST = Highstand Systems Tract, FSST = Falling-stage Systems Tract, LST = Lowstand Systems Tract, TST = Transgressive Systems Tract.

Fig. 15 - Incised valley generation and subsequent fill. (A) initial channel cut in response to base-level fall (falling-stage), (B) continued incision during base-level fall, (C-E) aggradation and lateral incision (widening) of the valley walls in response to base-level rises. Note all infill occurs during lowstand system tract.

Code	Facies	Description
A1	Grainflow facies	Predominately medium-grained white-yellow homogenous sands observed as steeply inclined packages (18° - 25°) up to 3 cm thick. Commonly compartmentalised by thinner packages of A3.
A2	Wind-ripple facies	Ripples up to 4 cm thick comprised of fine- to medium-grained extremely well-sorted sandstone, often lacking internal structure (translatent strata). Commonly interdigitates with facies A1 which it may grade laterally from.
A3	Grainfall facies	Thin (<4 mm) tabular packages of very well-sorted yellow-white fine sands that compartmentalise facies A1.
F1	Cross-bedded sandstone	Medium- to coarse-grained, moderate to well-sorted dark-red to red-brown sandstones arranged in planar- and tough-crossbedded sets that range from 0.4 - 4 m in thickness.
F2	Pebble-rich sandstone	Predominately clast supported conglomerate with medium- to coarse-grained sandstone dark red to red matrix. Clasts comprise angular to well-rounded clasts of small pebble to cobble size. Smeared mud clasts are sometimes evident, though often removed to leave elongate small voids (up to 3 cm long). Extra-basinal clasts of mafic and ultramafic origin are sporadic.
F3	Horizontal laminated sandstone	Fine- to medium-grained red-brown sandstone observed within channel bounding surface as 0.2 - 1 m thick sets or outside of the channel as 0.1 - 0.4 m thick sheets.
F4	Rippled sandstone	Very fine- to fine-grained, moderately sorted sandstone. Ripple strata exhibit sub-critical (<10°), critical and super-critical (24°) angles of climb. Ripple-forms have sinuous morphology. Shrinkage cracks, bioturbation and silty veneers are all common.
F5	Calcrete-rich sandstone	Very fine- to fine-grained, red to red-purple, moderately sorted sandstone. Contains abundant calcrete nodules and rhizoliths that can form complete calcrete horizons.
F6	Laminated siltstone	Red-brown to brown siltstone with subordinate mudstone arranged into thin horizontal laminations (<4 mm spacing). Commonly rooted and, or with sand-filled desiccation cracks.
F7	Massive sandstone	Red-brown to red, fine- to coarse-grained structureless sandstone.
F8	Wavy and convolute sandstone	Fine- to medium-grained, dark red to red-brown sandstone with wavy-like and or convolute lamination.
M1	Bioclastic limestone	Grey to dark grey bioclastic limestone with abundant <i>brachiopod</i> , <i>bivalve</i> , <i>bryozoan</i> , <i>crinoid</i> and coral fragments, no observed orientation. Facies frequently grades from, or to, facies M2.
M2	Siliciclastic-rich limestone	Dark grey limestone with up to 25% (by volume) of siliciclastic material. May contain shelly fragments of <i>brachiopods</i> , <i>bivalves</i> , <i>bryozoans</i> , <i>crinoids</i> and coral. Siliciclastic fraction comprises very fine- to coarse-grained sandstones.
M3	Fossiliferous grainstone	Light to dark grey small pebble to large pebble clast-supported conglomerate with very coarse-grained sandstone to gritstone matrix. Abundant broken fragments of shelly fauna. Grades vertically into facies M4. <i>Protichnites</i> , <i>Scolicia</i> and <i>Thalassinoides</i> trace fossils observed on some bedding surfaces.
M4	Coarse sandstone	Poorly sorted, angular to sub-angular, grey to light grey medium- to very coarse-grained sandstone with angular pebbles. Grades vertically from facies M3 in a upward-fining sequence.

Table 1. Characteristics of common lithofacies present in the lower Cutler beds.

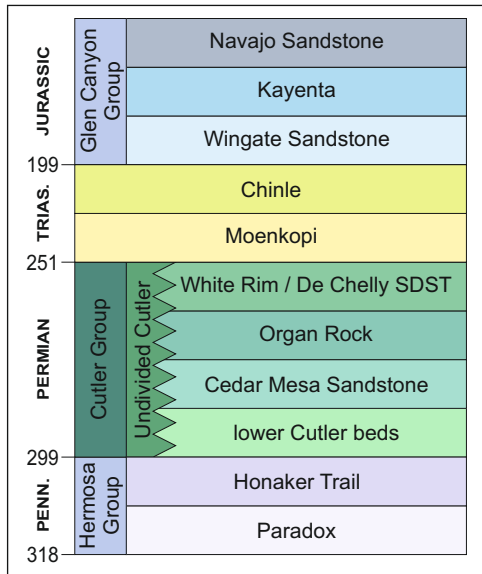


Figure 1. Summary stratigraphical chart for the Paradox Basin region.

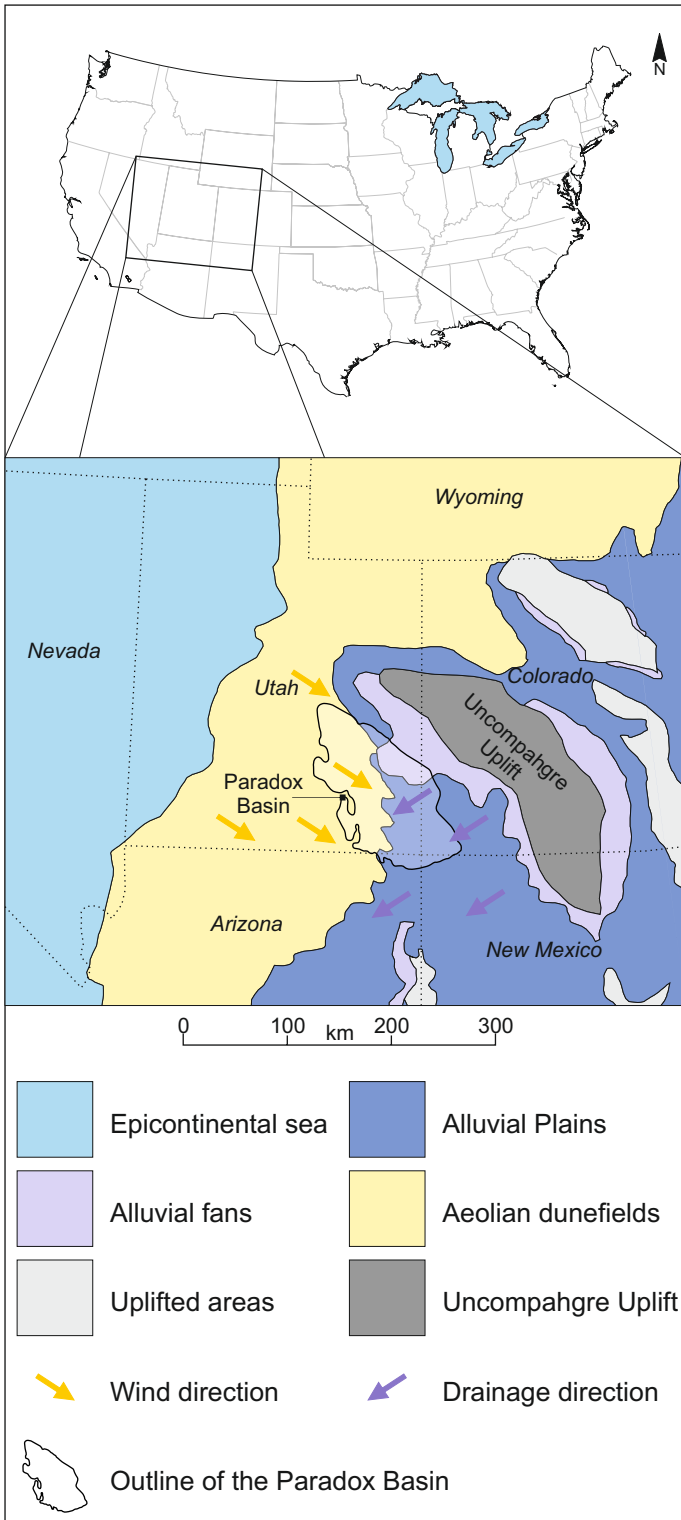


Figure 2. Summary palaeogeography of the Paradox Basin during the Sakmarian (~290 Ma). Modified in part after Blakey (2008).

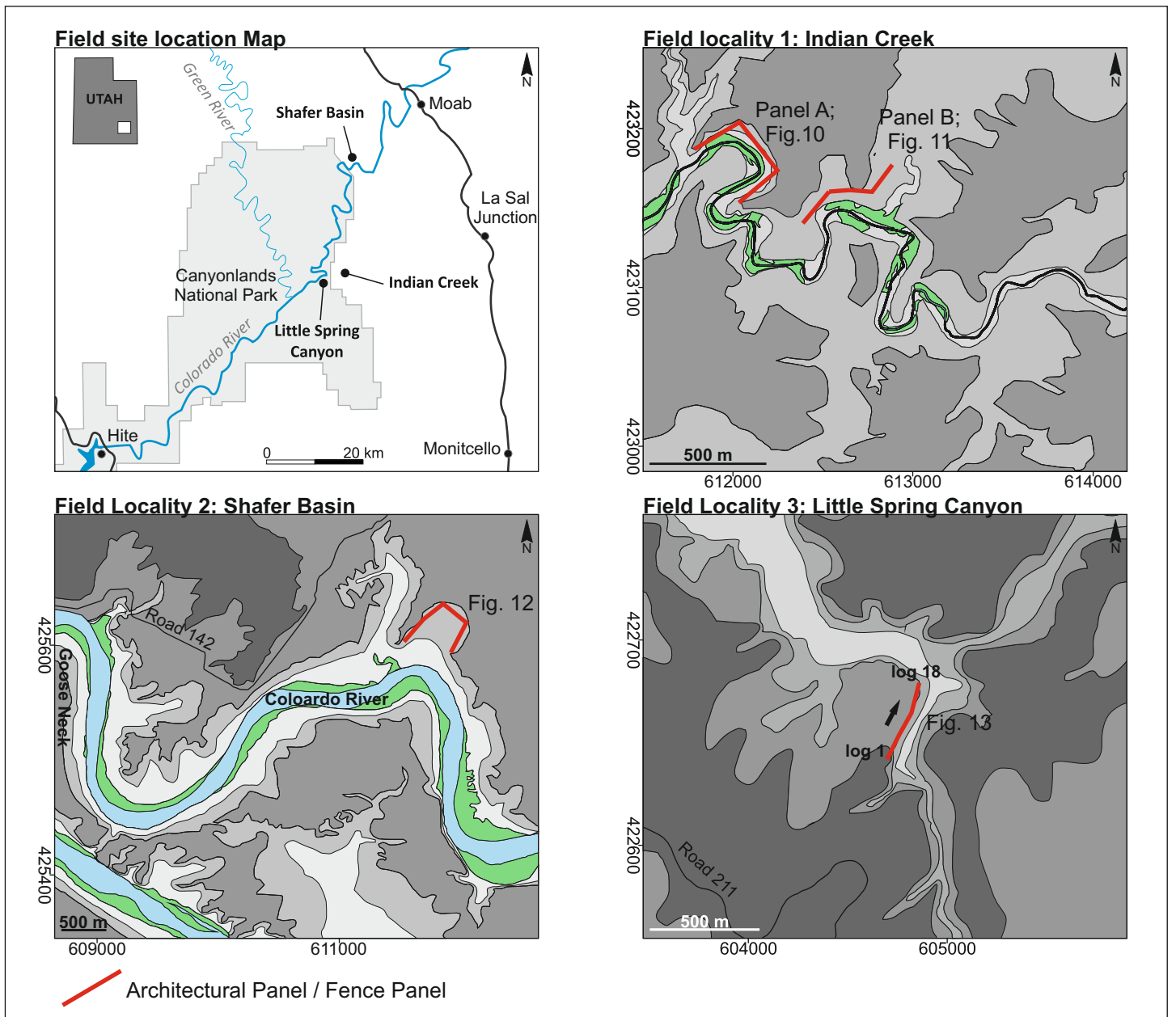


Figure 3. Field site location map (top-left) and individual location maps for the Indian Creek, Shafer Basin and Little Spring Canyon field localities. Darker grey colours depict areas of higher elevation in the field locality maps 1 - 3. Universal Transverse Mercator (UTM) co-ordinates shown.

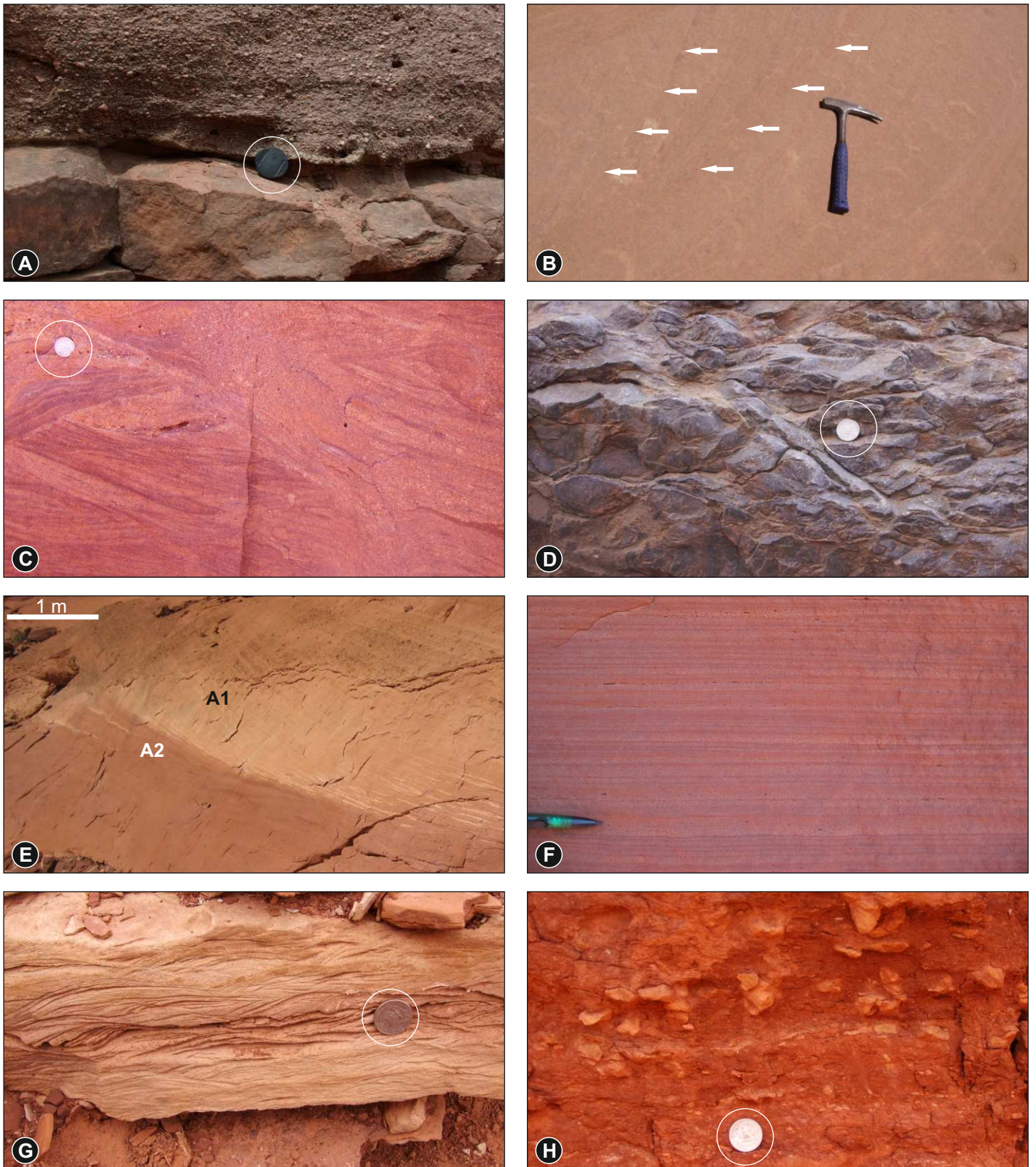


Figure 4. Example lithofacies of the lower Cutler beds. (A) Erosively based set of facies M3 (base of sheet-like granulestone barform element), overlying facies M4 (upper portion of sheet-like granulestone barform element). (B) Interbeds of facies A1 and A3 (aeolian dune element). Reactivation surfaces evident; depicted by arrows. (C) Compound co-sets of facies F1 (fluvial channel element). Outcrop cuts near perpendicular to palaeoflow direction. (D) Facies M2 showing highly nodular appearance (marine limestone element). (E) Toesets of facies A1 interfingering with facies A2 (aeolian dune and interdune elements). (F) Facies F3 exhibiting horizontal lamination and near-horizontal lamination (overbank element). (G) Fine-grained sets of facies F4 (fluvial channel element). (H) Immature palaeosol facies (F5) with root nodules (overbank element).

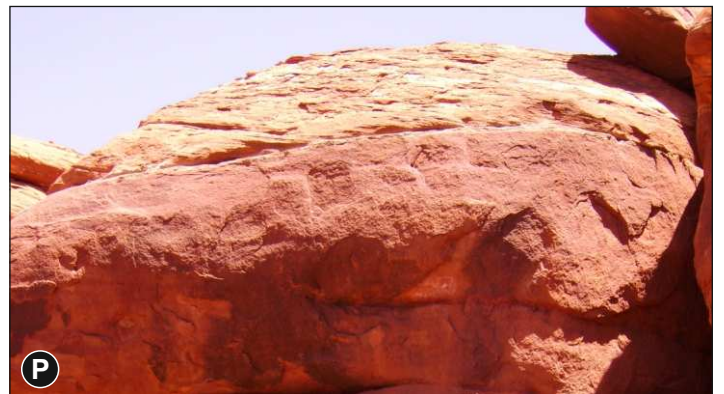
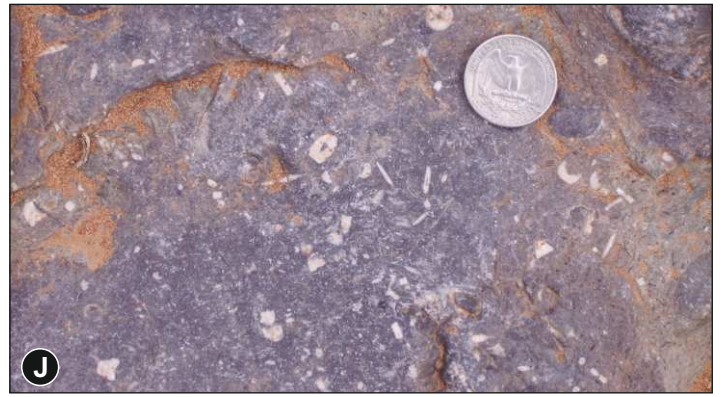


Figure 4 (continued). Example lithofacies of the lower Cutler beds. (I) Facies F2 with both intra- and extra-formational clasts present (basal component of fluvial channel element). (J) Bedding surface of facies M1 exposing broken shelly fauna (limestone bench element). (K) Desiccation cracks and rain-drop imprints of facies F8 (damp interdune element). (L) Close-up of facies M3 detailing grain size variation (granulestone barform element). (M) Cross-bedded sets of facies M4 (granulestone barform element). (N) Highly contorted unit of facies F8 (damp interdune element). (O) Interbeds of facies F5, F6 and F7 (overbank and interdune elements). (P) Facies A1 and A3 overlying a thick succession of F7 (aeolian sand dune overlying fluvial channel element).

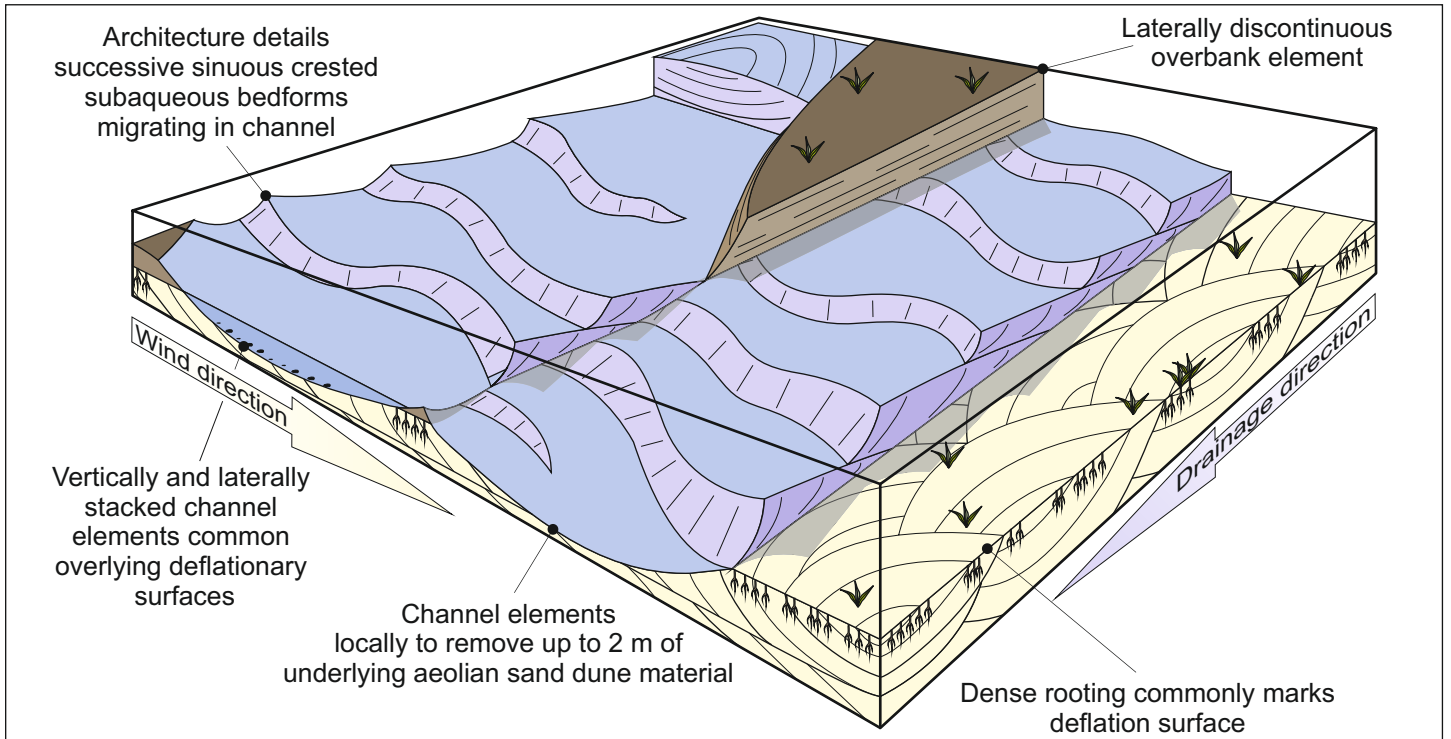


Figure 5. Model depicting the sedimentary architectural relationship between fluvial channel and aeolian sand dune elements.

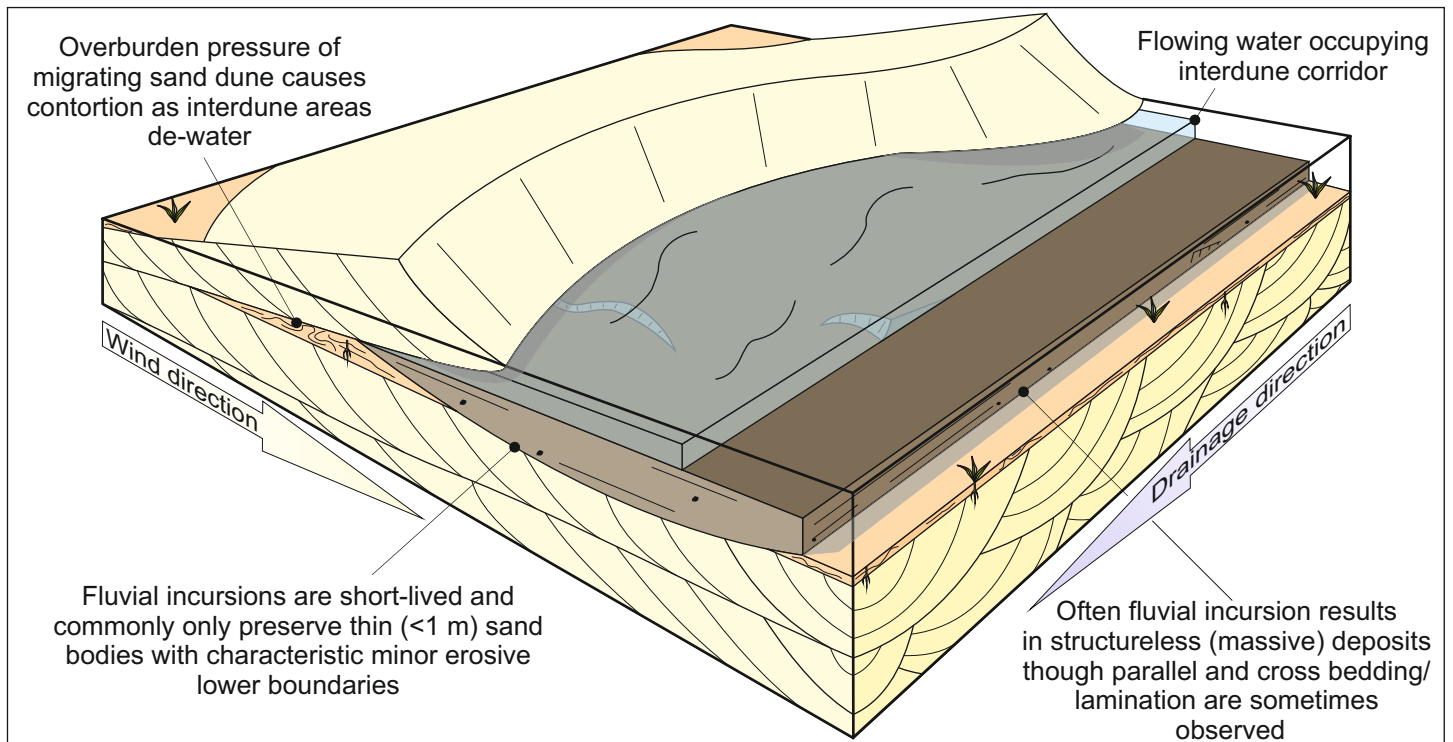


Figure 6. Model depicting the sedimentary architectural relationship between aeolian sand dune and wet interdune elements.

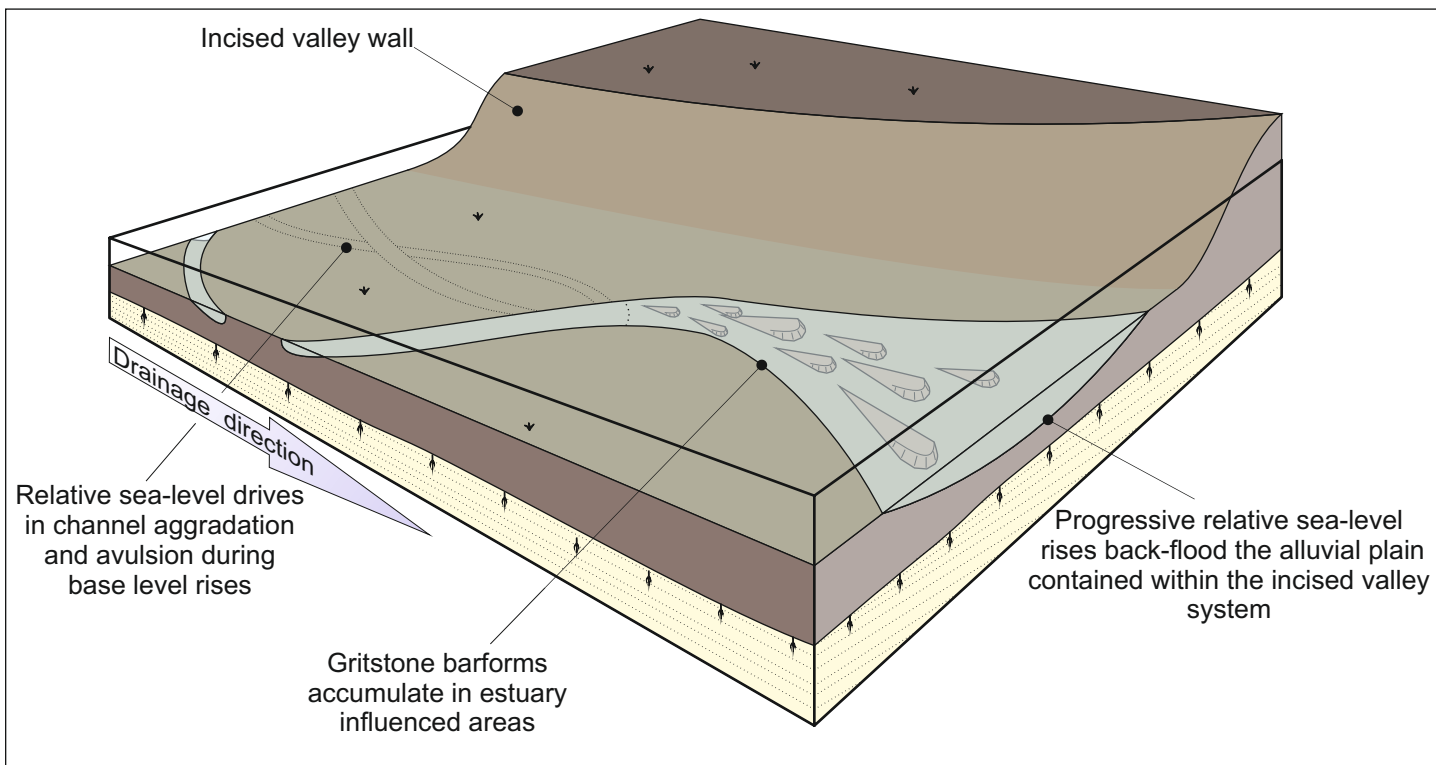


Figure 7. Model depicting the sedimentary architectural relationship between fluvial channel and granulestone barform elements.

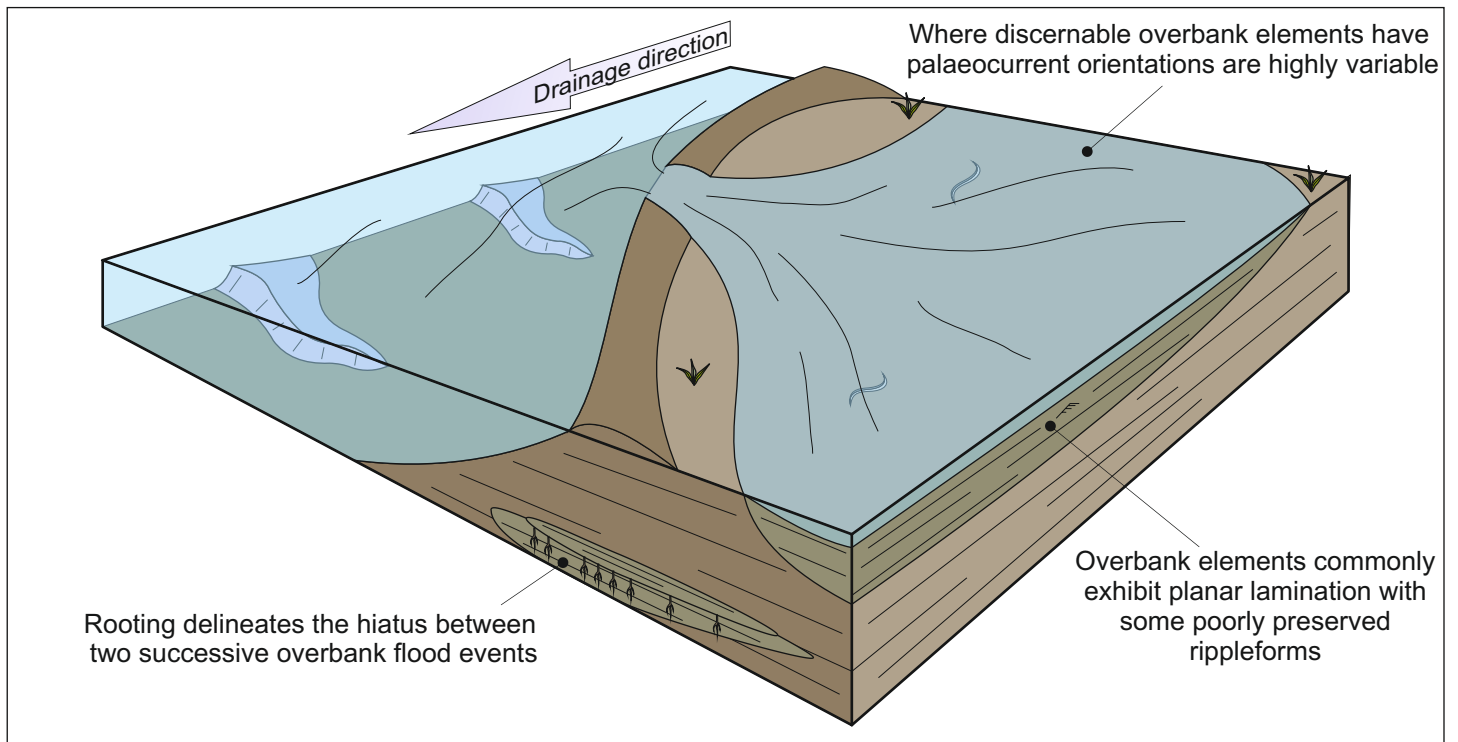


Figure 8. Model depicting the sedimentary architectural relationship between fluvial channel and fluvial overbank elements.

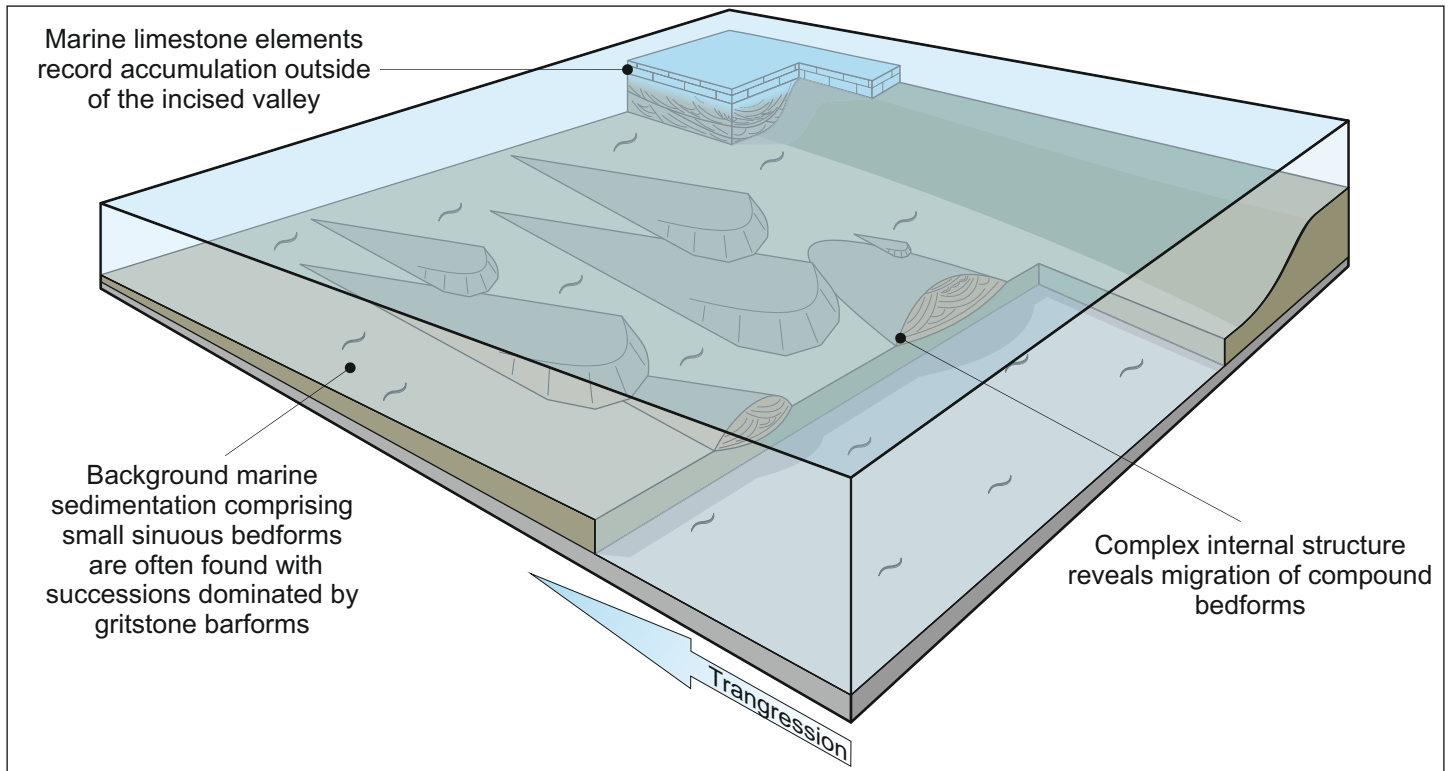


Figure 9. Model depicting the sedimentary architectural relationship between granulestone barform and limestone elements.

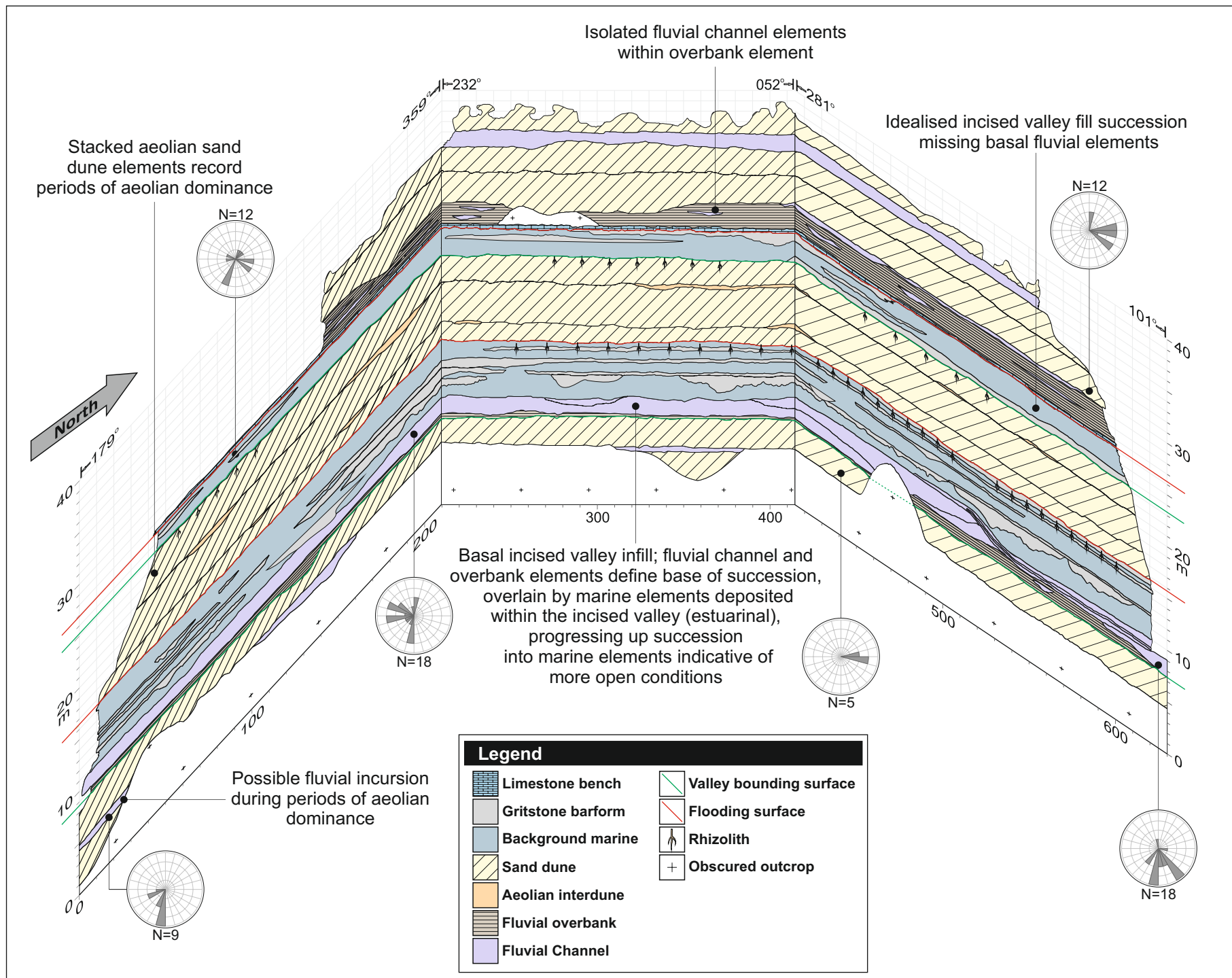


Figure 10. Architectural panel of lower Cutler beds at Indian Creek, Panel A. See Figure 3 for location.

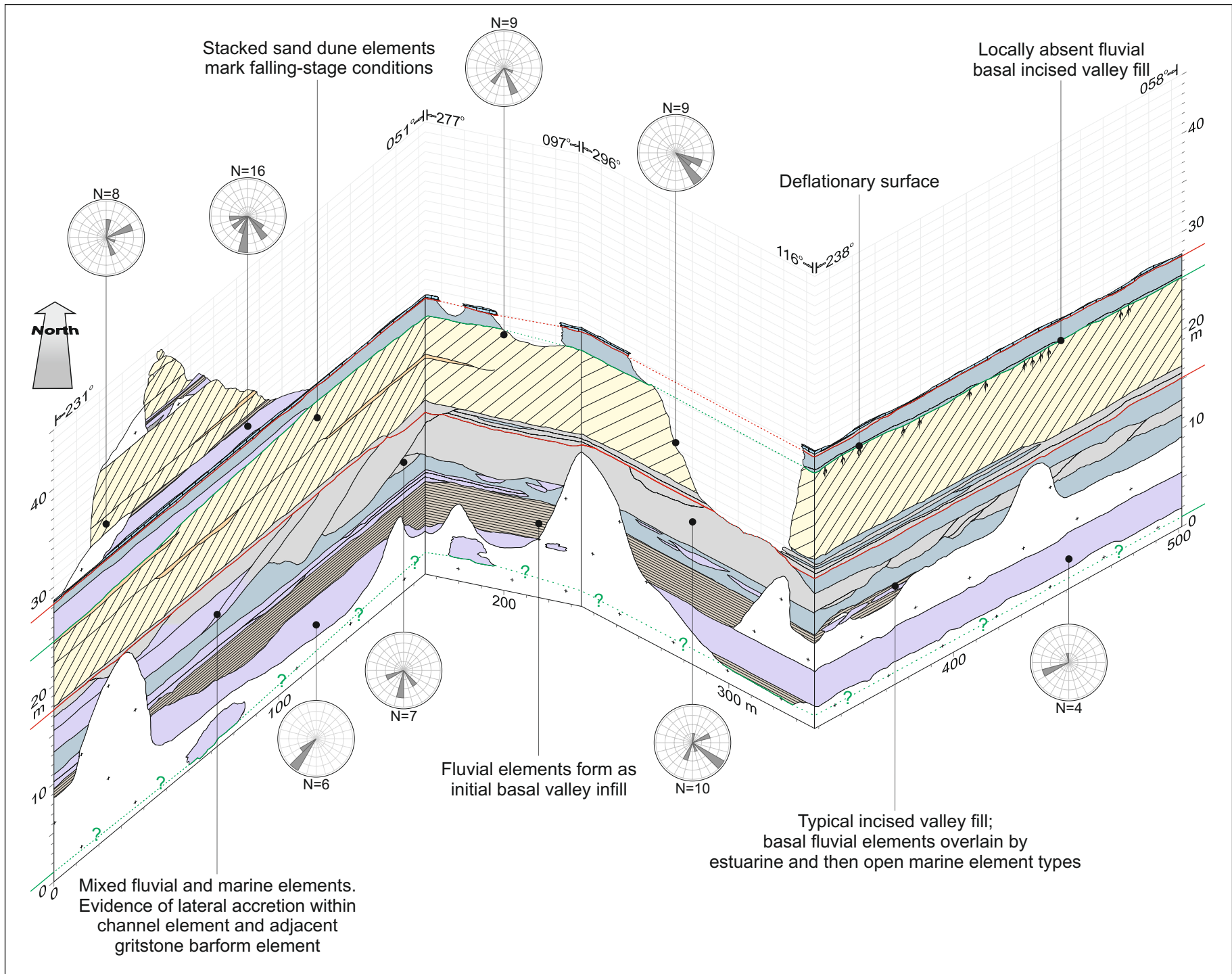


Figure 11. Architectural panel of lower Cutler beds at Indian Creek, Panel B. See Figure 3 for location.

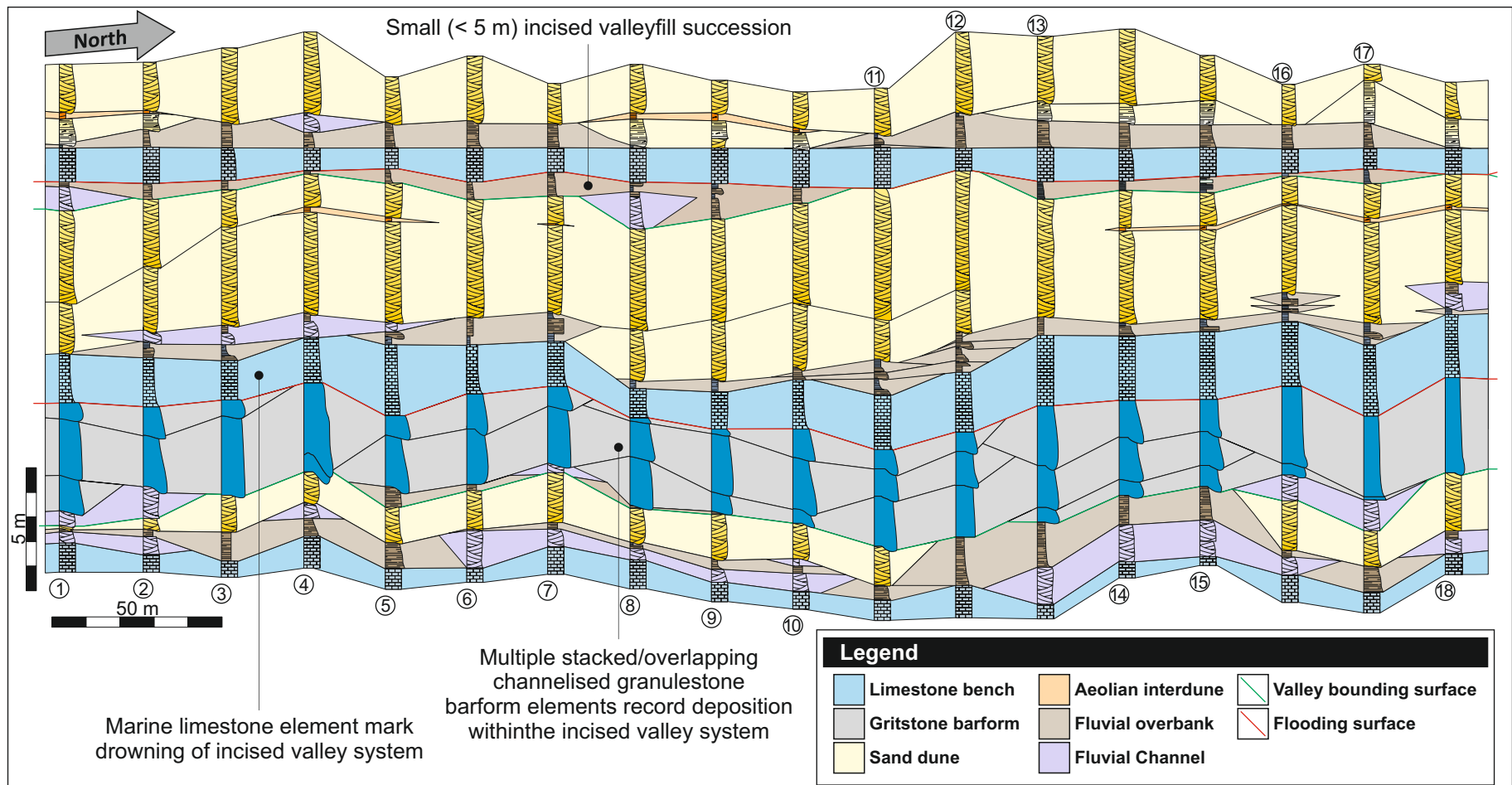


Figure 13. Little Spring Canyon correlation panel. Log correlations depict individual architectural elements. See Figure 3 for location. Individual sedimentary log grainsize increases towards the right.

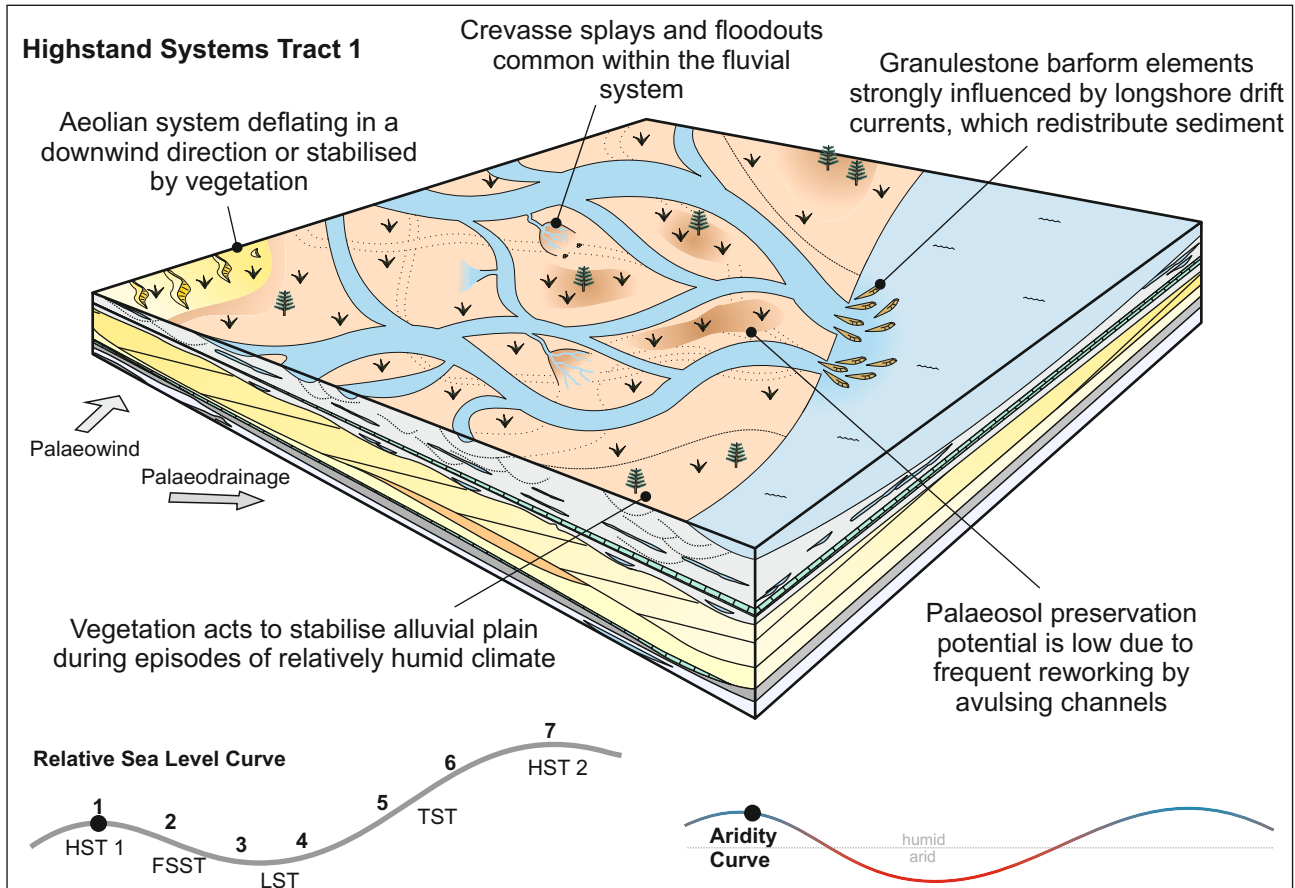


Figure 14a. Depositional and sequence stratigraphic model to account for the origin and style of infill of the incised valley systems present in the lower Cutler beds in response to combined relative sea-level and climatic change: Highstand systems tract 1. (A) highstand system tract; (B) falling-stage system tract; (C) late falling-stage system tract; (D) early low stand system tract; (E) middle lowstand system tract; (F) late lowstand system tract; (G) transgressive and highstand system tract. HST = Highstand Systems Tract, FSST = Falling-Stage Systems Tract, LST = Lowstand Systems Tract, TST = Transgressive Systems Tract.

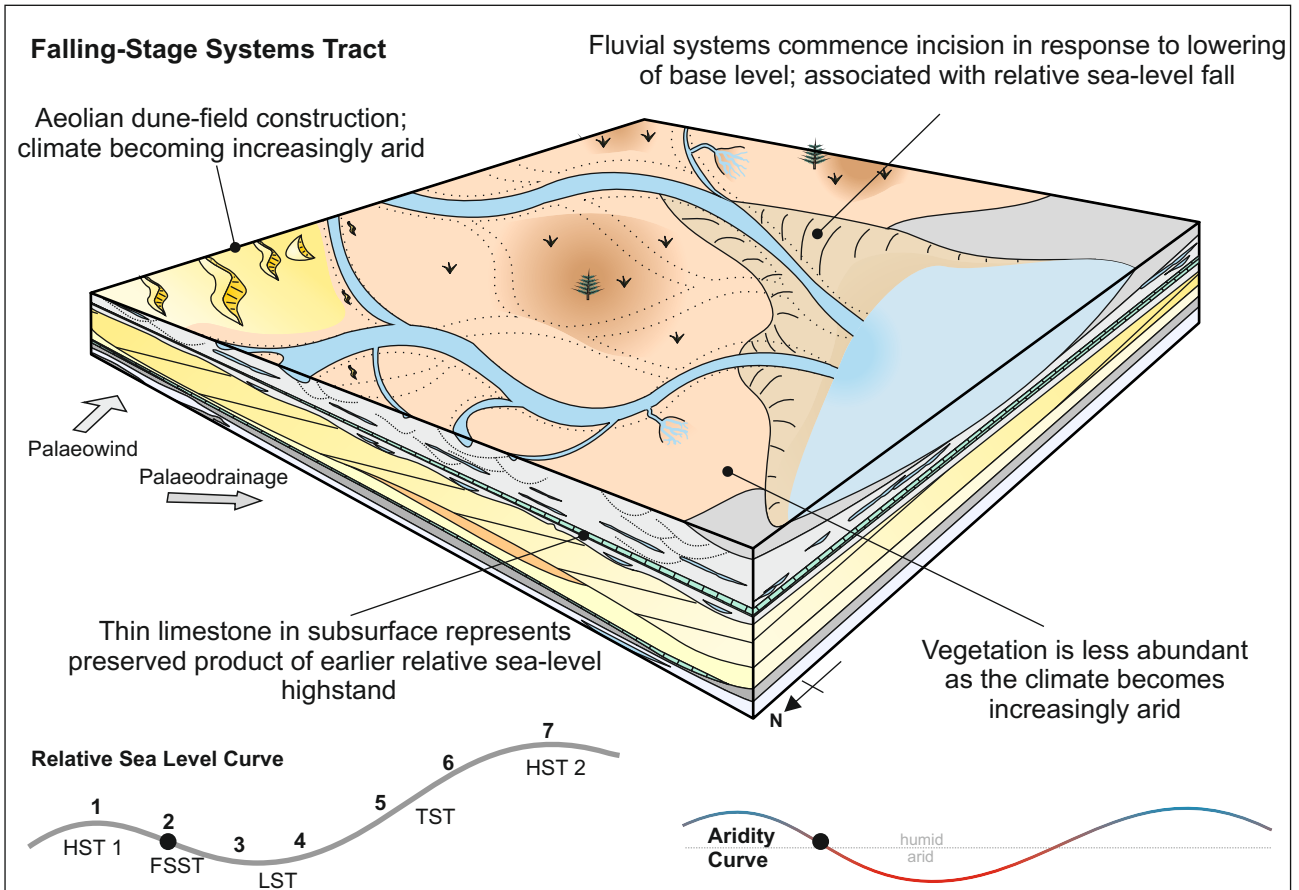


Figure 14b. Depositional and sequence stratigraphic model to account for the origin and style of infill of the incised valley systems present in the lower Cutler beds in response to combined relative sea-level and climatic change: Falling-stage systems tract (A) highstand system tract; (B) falling-stage system tract; (C) late falling-stage system tract; (D) early low stand system tract; (E) middle lowstand system tract; (F) late lowstand system tract; (G) transgressive and highstand system tract. HST = Highstand Systems Tract, FSST = Falling-stage Systems Tract, LST = Lowstand Systems Tract, TST = Transgressive Systems Tract.

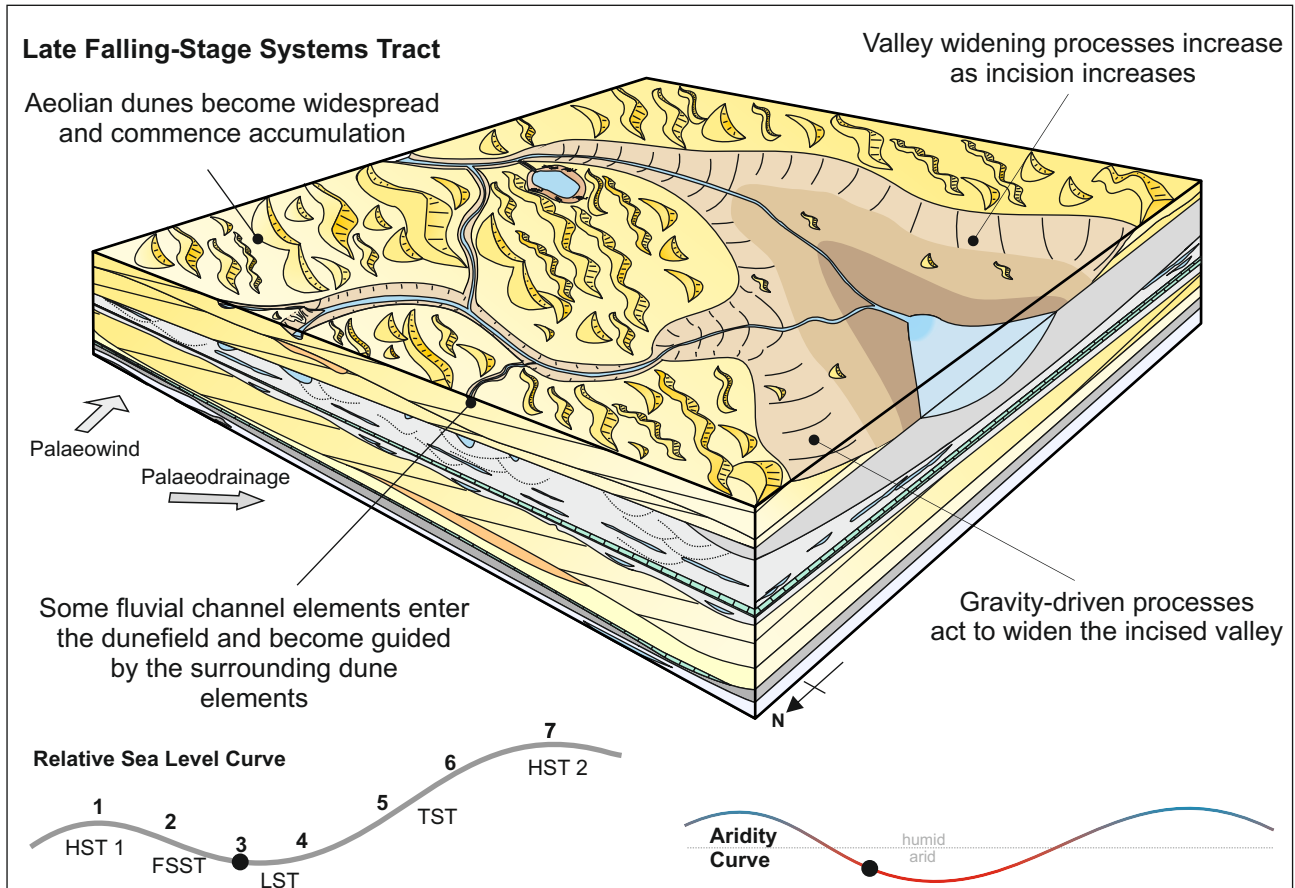


Figure 14c. Depositional and sequence stratigraphic model to account for the origin and style of infill of the incised valley systems present in the lower Cutler beds in response to combined relative sea-level and climatic change: Late falling-stage systems tract (A) highstand system tract; (B) falling-stage system tract; (C) late falling-stage system tract; (D) early low stand system tract; (E) middle lowstand system tract; (F) late lowstand system tract; (G) transgressive and highstand system tract. HST = Highstand Systems Tract, FSST = Falling-stage Systems Tract, LST = Lowstand Systems Tract, TST = Transgressive Systems Tract.

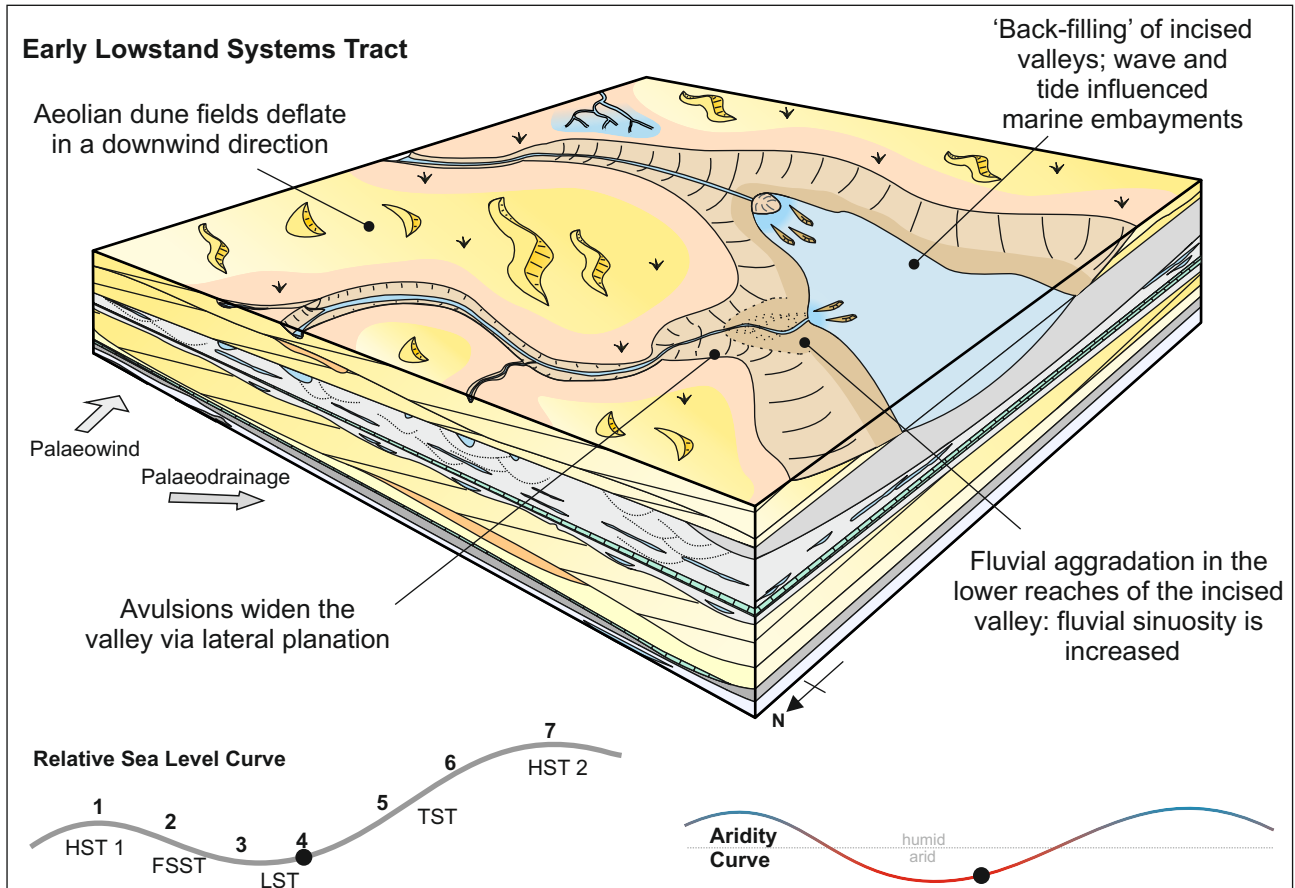


Figure 14d. Depositional and sequence stratigraphic model to account for the origin and style of infill of the incised valley systems present in the lower Cutler beds in response to combined relative sea-level and climatic change: Early lowstand systems tract. (A) highstand system tract; (B) falling-stage system tract; (C) late falling-stage system tract; (D) early low stand system tract; (E) middle lowstand system tract; (F) late lowstand system tract; (G) transgressive and highstand system tract. HST = Highstand Systems Tract, FSST = Falling-stage Systems Tract, LST = Lowstand Systems Tract, TST = Transgressive Systems Tract.

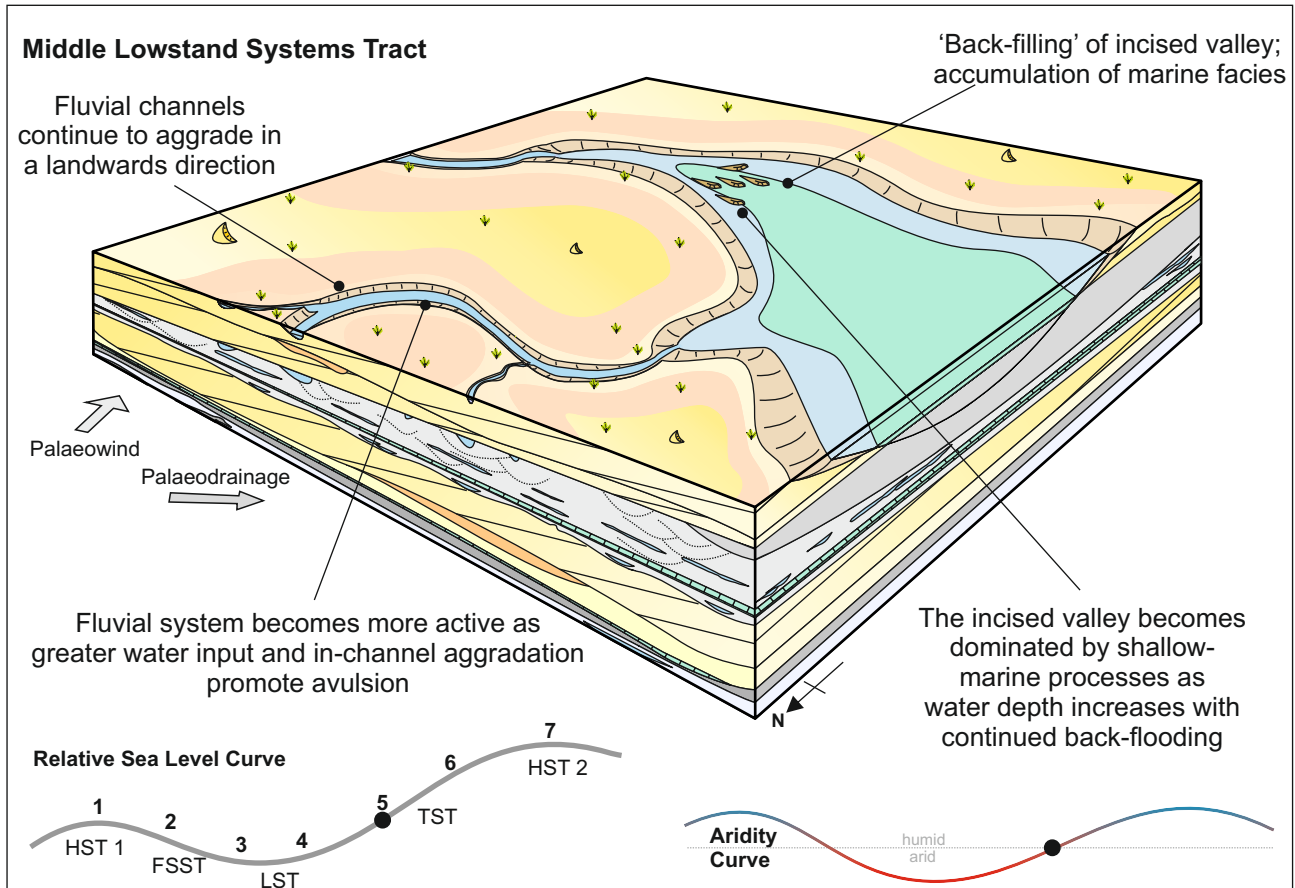


Figure 14e. Depositional and sequence stratigraphic model to account for the origin and style of infill of the incised valley systems present in the lower Cutler beds in response to combined relative sea-level and climatic change: Middle lowstand systems tract. (A) highstand system tract; (B) falling-stage system tract; (C) late falling-stage system tract; (D) early low stand system tract; (E) middle lowstand system tract; (F) late lowstand system tract; (G) transgressive and highstand system tract. HST = Highstand Systems Tract, FSST = Falling-stage Systems Tract, LST = Lowstand Systems Tract, TST = Transgressive Systems Tract.

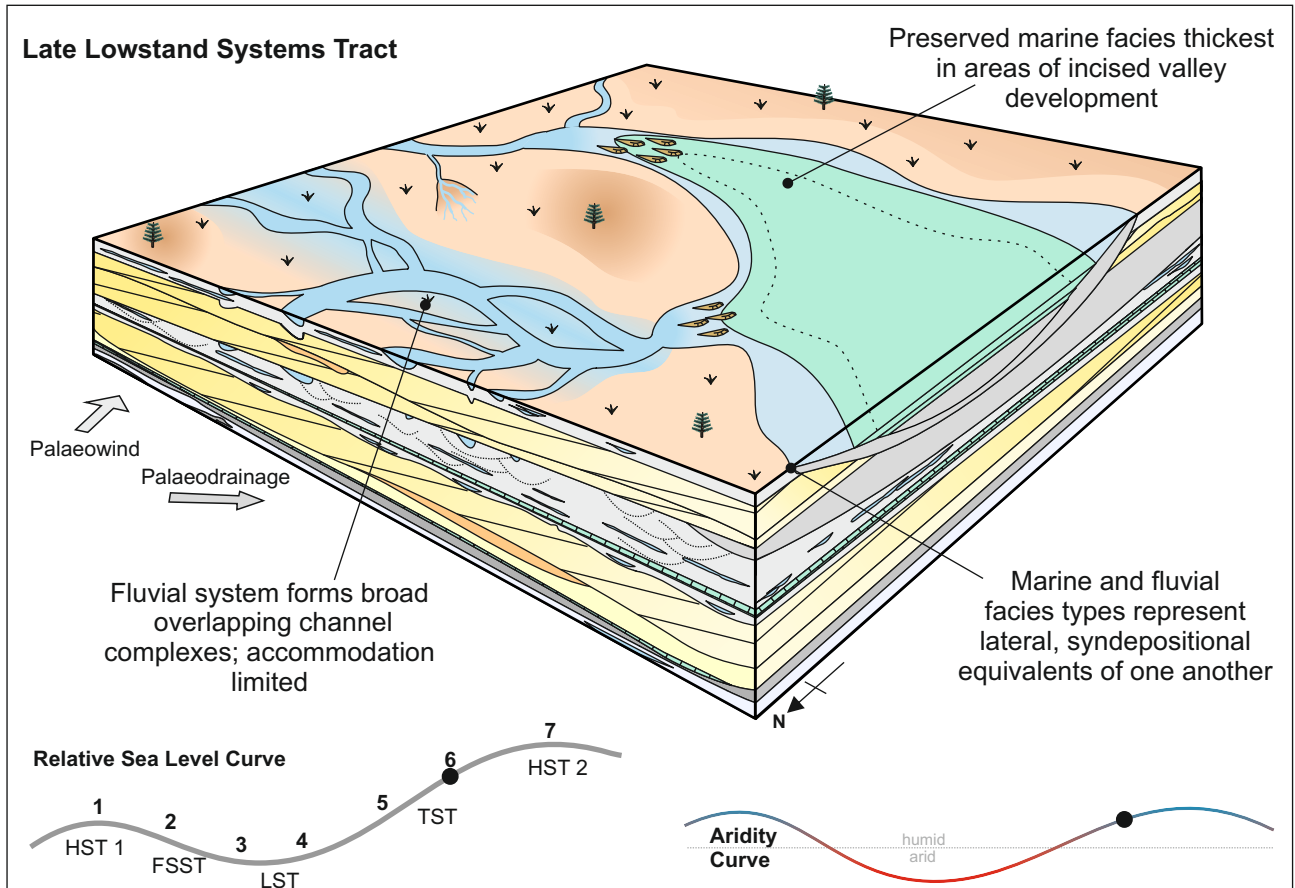


Figure 14f. Depositional and sequence stratigraphic model to account for the origin and style of infill of the incised valley systems present in the lower Cutler beds in response to combined relative sea-level and climatic change: Late lowstand systems tract. (A) highstand system tract; (B) falling-stage system tract; (C) late falling-stage system tract; (D) early low stand system tract; (E) middle lowstand system tract; (F) late lowstand system tract; (G) transgressive and highstand system tract. HST = Highstand Systems Tract, FSST = Falling-stage Systems Tract, LST = Lowstand Systems Tract, TST = Transgressive Systems Tract.

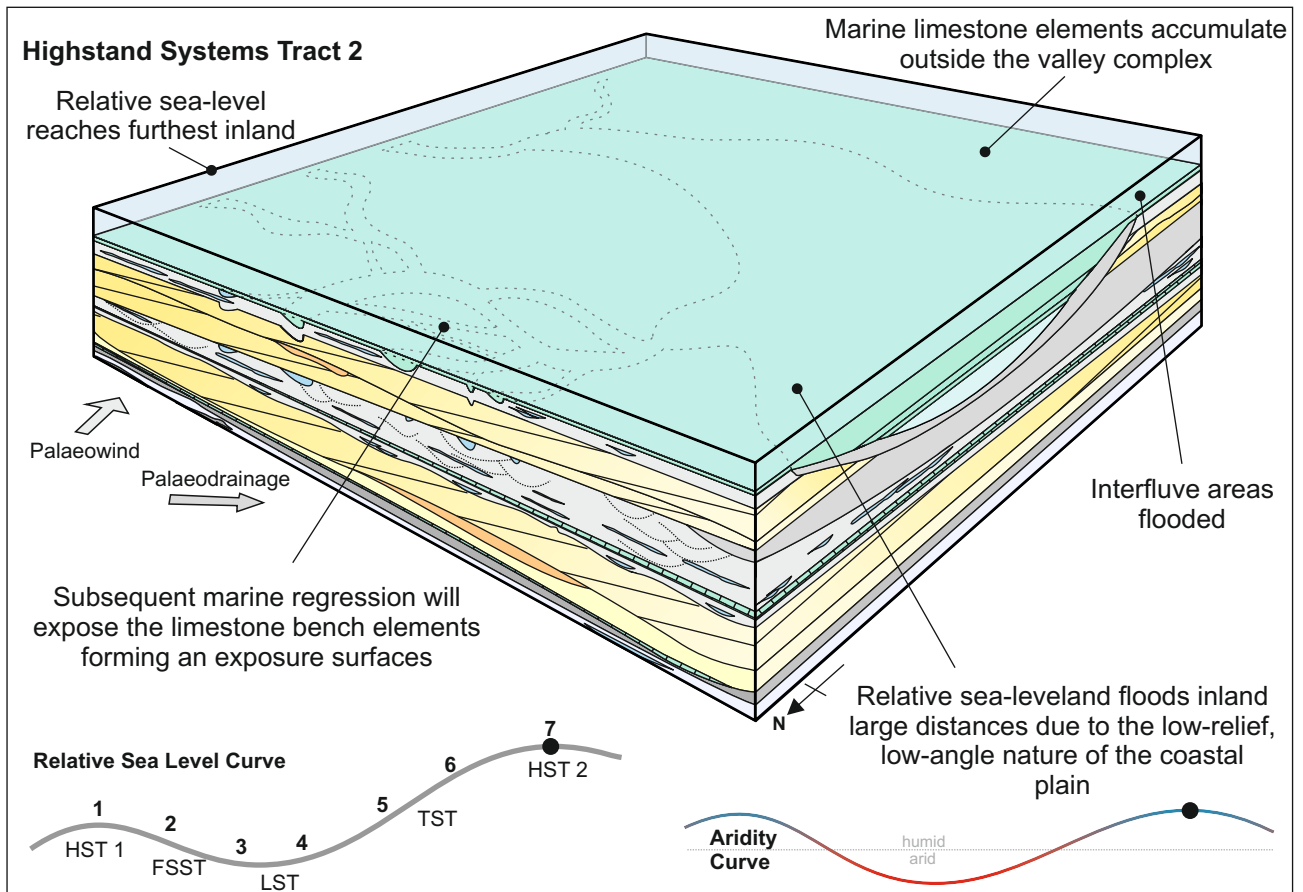


Figure 14g. Depositional and sequence stratigraphic model to account for the origin and style of infill of the incised valley systems present in the lower Cutler beds in response to combined relative sea-level and climatic change: Highstand systems tract 2. (A) highstand system tract; (B) falling-stage system tract; (C) late falling-stage system tract; (D) early low stand system tract; (E) middle lowstand system tract; (F) late lowstand system tract; (G) transgressive and highstand system tract. HST = Highstand Systems Tract, FSST = Falling-stage Systems Tract, LST = Lowstand Systems Tract, TST = Transgressive Systems Tract.

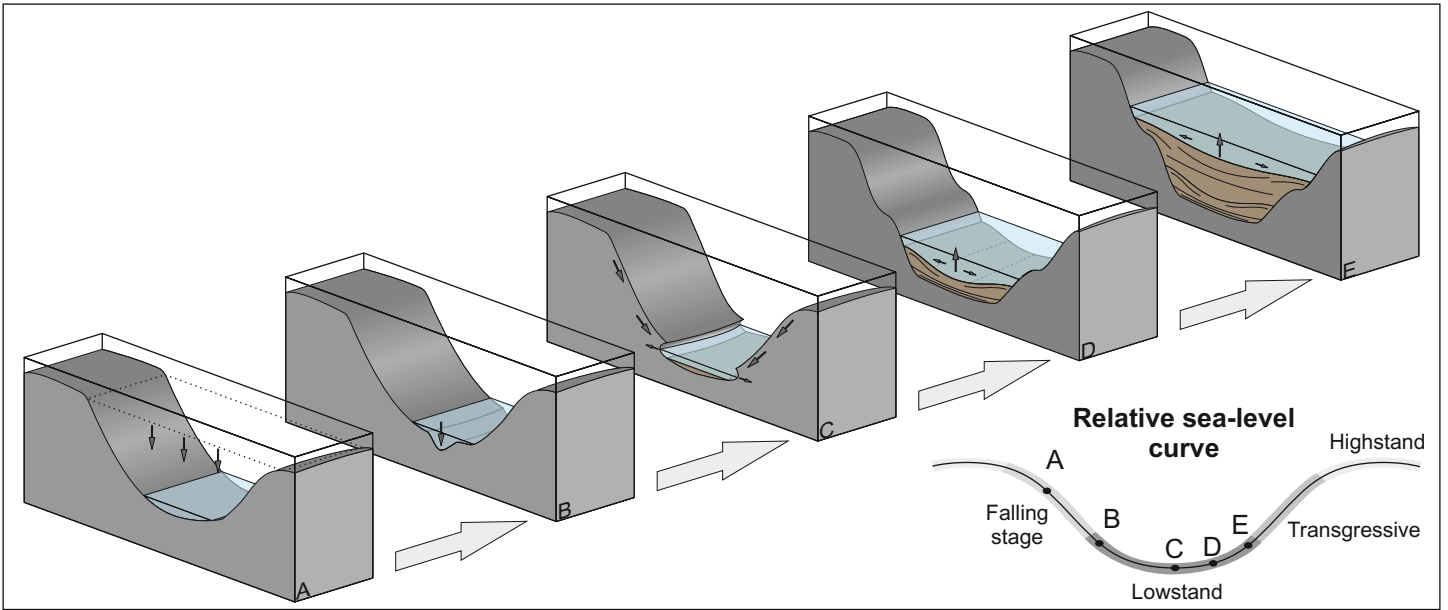


Fig. 15 - Incised valley generation and subsequent fill. (A) initial channel cut in response to base-level fall (falling-stage), (B) continued incision during base-level fall, (C-E) aggradation and lateral incision (widening) of the valley walls in response to base-level rises. Note all infill occurs during lowstand system tract.